Neural responses to the simulated 3D-orientation of rotating planes in area MSTd of the monkey.

Hiroki Sugihara

Department of Physiological Sciences,

School of Life Science,

The Graduate University for Advanced Studies,

Okazaki, Aichi 444-8585, Japan.

ABSTRACT

Motion is a powerful source of three-dimensional (3D) information about visual objects. For example, we can easily identify the structure of rotating objects solely on the basis of motion signals. This phenomenon is called Structure-From-Motion (SFM) perception. But the neural mechanisms underlying SFM have not been fully clarified. In the present study, I studied if the dorsal division of the medial superior temporal area (MSTd) in the macaque, which contains many neurons sensitive to complex motion stimuli, has activity related to SFM processing. As the simplest form of 3D structure, I chose a planar stimulus, and examined the relation between the neural responses and the simulated 3D-orientation of the plane defined by motion cues.

I recorded from 114 MSTd neurons while monkeys were performing a visual fixation task. These neurons responded to a basic set of optic flow patterns such as translation, expansion/contraction, and rotation. I examined responses of these neurons to rotating plane stimuli that were composed of random dots and that simulated rotating planes with various 3D-orientations. The simulated 3D-orientation can be characterized by two parameters, namely, tilt and slant, and I examined whether the MSTd neurons exhibited selectivity to these two parameters.

I found that most MSTd neurons tested (97 out of 114) responded to the plane stimuli, and many neurons (65 out of 97) exhibited selectivity to tilt and/or slant. Of 97 neurons, 18% (17/97) were selective only to tilt, 24% (23/97) only to slant, and 26% (25/97) to both. Certain stimulus components such as local translation, local speed, local speed gradients and distribution of velocities vary together with the change in the tilt and/or slant. However, control experiments have rejected the possibility that

selectivity is explained solely by the sensitivity to such components.

These results suggest that MSTd neurons are sensitive to stimulus features specific to the simulated 3D-orientation of the rotating plane stimuli and suggest that area MSTd is involved in SFM processing.

INTRODUCTION

One of the most important functions of the visual system is to recover three-dimensional (3D) information from the two-dimensional (2D) retinal image. There are various visual cues to recover 3D information; binocular disparity, shading, texture gradient, etc. Among these, motion is one of the most powerful cues. Actually, humans and macaques can easily perceive 3D structure of a moving object solely using 2D motion information contained in the projected image of the object (Siegel and Andersen 1988). For example, Wallach and O'Connell (1953) showed that people who saw the projected shadows of wireframe figures could easily perceive the 3D structure of the wireframe. When the figure was stationary, the shadow appeared as 2D pattern, but as soon as it started to move (rotate), the shadow could suddenly pop out in depth and was perceived as a solid object rotating in 3D space. This phenomenon is called Structure-From-Motion perception.

Then, how can 2D-motion information induce perception of 3D structure? Some spatial distributions of 2D motion vectors may contribute to 3D perception. Specifically, speed gradient may be an important possibility. If an observer on the ground surface sees his side while moving ahead, speed gradient (motion parallax) is generated in the retinal image that contains a singular point with zero velocity which corresponds to the gaze direction. If the speed of the observer is constant, the speed gradient and the slant of the ground surface have a fixed relationship in which higher motion gradient indicates steeper slant. Thus, in such a case, the speed gradient is a useful clue to recover the environmental structure, the surface slant. Actually, humans can have depth perception from the speed gradient (Braunstein 1968; Harris et al. 1992).

The same relationship between the speed gradient and the surface slant exists in the case of object motion, i.e. SFM. In the case of SFM, however, the object contains many local speed gradients with multiple directions. Thus, to recover the global structure of the object, further integration of local speed gradients should be required.

Next, what kind of neural mechanism underlies SFM? There are two parallel pathways in the visual cortex (Ungerleider and Mishkin 1982). One is the ventral pathway, which starts from the primary visual cortex (V1) and goes to the inferior temporal cortex. The ventral pathway is believed to be involved in processing of shape and color. The other pathway is the dorsal pathway, which starts from V1 and goes to the posterior parietal cortex (Fig. 1). It is believed that motion information is processed in the dorsal pathway. In the primate, selective responses to motion first emerge in V1. Directionally selective V1 neurons preferentially respond to motion in a particular direction within a small receptive field (Fig. 1). Because single V1 neurons can only deal with motion signals through small apertures, it is unlikely that they process SFM in an explicit fashion. V1 sends its outputs to several extrastriate areas including MT. In area MT, many neurons have direction selectivity and some neurons are also selective to the direction of speed gradient (Treue and Andersen 1996; Xiao et al. 1997). Area MT is believed to be specialized for motion processing. Several electrophysiological studies of the macaque monkey have examined the contribution of area MT to the processing for SFM. Bradley et al. (1998) employed a moving random-dot pattern that is perceived as a rotating cylinder and found that the responses of MT neurons changed with the change in the perceived structure of the motion stimulus. Lesions in area MT were shown to prevent the perception of SFM (Andersen et al. 1996). These reports suggest the involvement of MT in the processing

of SFM.

MT neurons, however, have relatively small receptive fields and preferentially respond to locally presented translational motion stimuli. This response property might be suitable for some kinds of structural processing, such as the depth-order assignment of motion-transparent surfaces (Bradley et al. 1998; Qian and Andersen 1994). However, it is doubtful that a single MT neuron can code more complex structures, such as those with multiple motion gradients in various directions. Because even simple SFM stimuli like a rotating cylinder are actually composed of complex patterns of motion gradients, spatial integration of local motion signals seems essential for the processing for SFM. It has been proposed that the processing of SFM consists of multiple stages (Hildreth et al. 1995) and the integration of local motion signals may take place beyond area MT.

The dorsal division of the medial superior temporal area (MSTd), which is located in the upper bank of the superior temporal sulcus, receives a direct projection from MT (Maunsell and Van Essen 1983; Ungerleider and Desimone 1986). Neurons in MSTd have large receptive fields and respond selectively to complex stimuli such as expansion, contraction and rotation (Duffy and Wurtz 1991; Graziano et al. 1994; Lagae et al. 1994; Raiguel et al. 1997; Saito et al. 1986). Recently, an fMRI study in human subjects reported that responses related to SFM perception occurred in MT+, which is considered to be homologous to macaque areas MT and MST (Orban et al. 1999).

In the present study, I recorded the activity of MSTd neurons and studied its relation to SFM processing. In order to relate neural responses to SFM processing, the response selectivity to the simulated 3D structure of a surface was examined. I employed a rotating plane, inclined in a particular 3D-orientation (plane stimulus), as an

SFM stimulus (Fig. 2A). The plane stimulus was composed of random dots having a limited lifetime, and was perceived vividly as a 3D-oriented surface in spite of the absence of depth cues other than motion. I employed this stimulus because it is well established that MSTd neurons respond to rotating frontoparallel planes and I thought that MSTd neurons might also respond to the rotation of variously 3D-oriented planes. Furthermore, this stimulus is appropriate for a quantitative study because the structure of this stimulus can be defined by only two parameters, namely, tilt and slant (Fig. 2B). If area MSTd is involved in SFM processing, MSTd neurons should exhibit selectivity to these structural parameters.

In the current study, I find that many MSTd neurons have selectivity for tilt and/or slant of the rotating plane stimulus. The selectivity is position-invariant as well as speed-invariant. These results indicate that the selectivity of MSTd neurons to the rotating plane cannot be explained simply as responses to the local motion components of the plane stimulus, but rather as responses to the global stimulus. Thus, MSTd neurons can code the 3D structure of rotating planes and this suggests that area MSTd is involved in SFM processing.

METHODS

Behavioral task

Recordings were made from 3 awake, Japanese monkeys (*Macaca fuscata*). All procedures for animal care and experiments were in accordance with the NIH Guide for the Care and Use of Laboratory Animals (1996) and were approved by the animal experiment committee of the Okazaki National Research Institutes.

During the experiments, each monkey sat in a primate chair and looked at the CRT monitor (SONY GDM-2000TC) binocularly (Fig. 3). The monitor was placed approximately 32 cm in front of the monkey so that 1 deg corresponded to 15 pixels (approximately 0.55 cm) and the monitor covered 68.3 deg x 51.2 deg. (Hereafter "deg" will be used to refer to the degree of visual angle.) Each monkey was trained to perform a fixation task (Fig. 4). A trial started when a small fixation spot appeared on the monitor. The monkeys were required to foveate the fixation spot within 500 ms and to maintain its gaze within 1 deg x 1 deg (or occasionally 4 deg x 4 deg) window. At the end of a successful trial, a drop of water was delivered as a reward, the fixation spot was turned off, and a 2 s intertrial interval was initiated. Eye position, both of vertical and horizontal, was monitored with the sampling rate of 1 kHz using the magnetic search coil technique (Robinson 1963). If the monkey's eye deviated beyond the window during a trial, the trial was automatically terminated without a reward and the intertrial interval was initiated. During the period of fixation, a visual stimulus was presented. Data collection, events for the fixation task, and stimulus presentation were controlled by computer (Fig. 3).

Surgery and recording

A stainless steel recording chamber and a head holder were fixed to the skull under general anesthesia and sterile surgical conditions. A search coil was placed in the eye and was connected to a plug on the top of the skull. After surgery, the monkey was allowed to recover for at least 1 week before the experiment began. During this period, antibiotic (Cefazolin sodium) was given every 12 hrs.

Single-neuron activity was recorded from MSTd. The recording chamber was placed over the occipital cortex for one monkey and over the parietal cortex for two monkeys. A glass-coated Elgiloy microelectrode or varnish-coated tungsten microelectrode was advanced through the dura or inside a stainless steel guide tube that was advanced manually through the dura. Extracellular action potentials were amplified and single neuron activity was isolated with a time-amplitude discriminator. Spike times were then converted to pulse sequences. MSTd was identified based on the following criteria: 1) depth below the dura, 2) location relative to area MT, 3) selectivity for optic flow, and 4) receptive field (RF) size.

The RF of an MSTd neuron was roughly mapped by a stimulus of the basic stimulus set (see below). The RF typically contained the foveal region and usually covered the contralateral half of the CRT monitor and extended into the ipsilateral side to a considerable extent.

Visual stimuli and selectivity test

Every neuron was tested with two sets of stimuli. Stimuli were presented at the center of the RF. Within each set, visual stimuli were presented in a pseudorandom interleaved fashion, one stimulus per trial, and each stimulus was repeated at least four

times, usually more than five times. Each stimulus consisted of 60 frames of moving random dots. The size of each dot is approximately 0.07 deg x 0.07 deg. Each frame of the stimulus was generated during the intertrial interval, stored in the computer memory, and presented in sequence during stimulus presentation. The position of the dots varied across trials. During testing, the movies were presented at a frame rate of 60 Hz. Each stimulus had a duration of 1 s. The neuron's baseline activity was measured during 400 - 0 ms before the stimulus presentation. The visual response was defined as the mean discharge rate during stimulus presentation minus the baseline activity.

1. Basic stimulus set

The first set consisted of eight stimuli to test selectivity for basic optic flow patterns: expansion, contraction, clockwise rotation, counterclockwise rotation, and the four directions of translation (up, down, right, and left) (Fig. 6). Each stimulus was composed of 314 dots that were displayed within a circular window (26.7 deg in diameter). Each dot moved for a 150 ms lifetime, disappeared, and then appeared at a new random location within the circle, and was given a trajectory and speed appropriate to its new location. The dots were relocated asynchronously, to avoid a coherent flickering of the stimulus. This constant reshuffling virtually eliminated pattern artifacts because the pattern of the dots was constantly and randomly changing. The reshuffling also eliminated density artifacts, since each local region in the display had approximately the same number of dots at any time. As a result, the mean luminance was also constant across the display. The translational motion stimuli moved at 20 deg/s, which is equal to the average dot speed in the expanding, contracting, and rotating stimuli.

2. Plane stimulus set

The second stimulus set consisted of rotating planes in various simulated 3D-orientations (Fig. 2C). Each stimulus in this set was also composed of random dots, but their velocity field simulated a rotating plane. A simulated 3D-orientation was defined by two parameters, tilt and slant (Fig. 2B). The tilt is defined as the orientation of the projection of the surface normal on the frontoparallel plane. In this report, 0° of tilt corresponds to rightward and 90° of tilt correspond to upward in the tilt-slant space (Fig. 2C). The slant is defined as the angle between the surface normal and the line of sight. In mathematical terms, different orientations of the plane stimuli can be represented as combinations of rotation and deformation with various ratios (Koenderink 1986). Such a description may be more neutral than the description using terms like 'tilt' and 'slant' that are intimately related to the 3-dimensionality of an object. However, the description of the stimuli using such mathematical terms is less intuitive. Thus, in the following, I will use the terms 'tilt' and 'slant' to characterize different stimuli for the sake of simplicity. I used a set of four tilts, namely, 0°, 45°, 90°, and 135°, and a set of four slants, namely, 0°, 20°, 40°, and 60° (Fig. 2C). 0° of slant corresponds to a plane rotating on the frontoparallel plane and the tilt cannot be defined. The plane stimulus set consisted of the combinations of each slant and tilt, thus, a total of 13 stimuli (4 tilts × 3 slants + 0°-slant stimulus). The pattern was rotated about the surface normal vector passing through the center, at 28 revolutions per minute (rpm). The direction of rotation that elicited the better response in the basic stimulus set was employed for plane stimulus set. The opposite direction of rotation was also examined in many neurons. For the stimulus with slant equal to 0°, the average dot speed was 20 deg/s, which was equal to the average speed in the basic stimulus set. To avoid a

change in the spatial extent of the stimulus pattern accompanying the change in simulated 3D-orientation, a circular aperture of 26.7 deg in diameter was used (Fig. 2A). So, all the stimuli in the plane stimulus set had the same spatial extent as those in the basic stimulus set. This made the average speed larger for stimuli having steeper slants. Positions of the dots were calculated using orthographic projection to remove perspective information; no disparity information was added. Because of the orthographic projection, the stimuli had an ambiguity with respect to tilt such that two stimuli having a tilt difference of 180° were identical to each other. Other properties of the stimuli in the plane stimulus set were the same as those of the basic stimulus set.

To quantify the selectivity for the plane stimulus set, the best stimulus (i.e., the one that generated the maximum response) was first identified among the plane stimulus set. If the best stimulus was the 0°-slant stimulus, for which tilt is not defined, the second best stimulus was taken as the best in order to quantify the tilt selectivity. In all but one such cases, the second best stimulus was the 20°-slant stimulus. Next, the slant selectivity was examined among the stimuli that had the same tilt as the best stimulus. Neurons were classified as slant selective if the responses varied significantly among the stimulus family having the same tilt (one-way ANOVA, $p < 0.05$). Similarly, I examined the tilt selectivity across all the stimuli that had the same slant as the best stimulus. I also calculated tilt or slant selectivity index to evaluate the degree of selectivity. The selectivity index was calculated by using the minimum and the maximum response in the responses used in ANOVA : 1 - (minimum response) / (maximum response). Because each response was described relative to the baseline activity, the minimum response was negative when inhibitory, making the selectivity index greater than one.

For some of the neurons that exhibited slant selectivity or tilt selectivity, three additional stimulus sets, described below, were used for control experiments to examine if the selectivity could be explained as the tuning to local translational motion, local speed, local speed gradients or distribution of velocities.

Control 1. Position invariance

The first stimulus set in the control experiment aimed to test the effect of the direction of local translational motion. The best stimulus in the plane stimulus set was presented at five retinal locations within the RF (Fig. 16). The stimulus size was the same as those of the main experiment. Five stimulus positions lay in an overlapping cloverleaf arrangement (Fig. 16A) and, as a whole, covered 53.4 deg (51.2 deg vertical, due to the limit of the CRT monitor size). The central position was the same position as that used for the plane stimulus set. In the regions where the different stimuli overlapped, the direction of local motion reversed even if the entire extent of the stimuli were rotating in the same direction. Therefore, if a neuron responded in the same way at all five positions, the response cannot be explained by tuning to the direction of local translational motion. In addition to the best stimulus, a stimulus with the same slant and tilt as the best stimulus but with the opposite direction of rotation was also used. Thus, each cell was given a total of 10 different stimuli (5 positions $\times$ 2 rotations). To examine the position invariance of the responses, I compared selectivity for direction of rotation across the five positions (Graziano et al. 1994).

Control 2. Rotation speed

The second stimulus set in the control experiment aimed to test the effect of the speed of the moving dots. Because I employed the same circular aperture for every stimulus in the plane stimulus set, the maximum or average speed as well as the magnitude of the

speed gradient contained in the stimuli increased with the increase of slant. This may cause an apparent selectivity for slant if the neuron examined is sensitive to dot speed. To examine such a possibility, I tested slant selectivity using three rotation speeds; slow (19 rpm), standard (28 rpm), and fast (42 rpm). Every stimulus had the same tilt as the best stimulus in the plane stimulus set. If the selectivity to slant does not change with the change in rotation speed, selectivity for the plane stimulus set cannot be explained by sensitivity to speed.

Control 3. Shuffled plane stimuli

The third stimulus set in the control experiment aimed to test whether the neurons are really sensitive to the structure of the velocity field. An alternative possibility is that the neurons simply respond to the distribution of velocities regardless of their spatial configuration. As a control for such possibility, I prepared another stimulus set by randomly shuffling the locations of dots from the original plane stimulus preserving their velocities (shuffled stimulus). Thus, the shuffled stimuli contain the same distribution of velocities with the original plane stimulus, but have no 3D information. If the neurons are really sensitive to slant and/or tilt, I can expect that the neurons will lose selectivity to the stimulus set or will not respond at all.

Histology

Upon completion of the last recording session, all of the three monkeys were euthanized under deep anesthesia with sodium pentobarbital and perfused through the heart with saline followed by 4% paraformaldehyde. The brain was then removed from the skull, sectioned (50 μm in thickness) in the parasagittal plane. For two monkeys, their sections of brains were stained with cresyl violet. Damage from the

insertion of the guide tubes was identified at the anterior bank of the superior temporal sulcus and the locations corresponded well with the location of MSTd as described previously (Komatsu and Wurtz 1988). For the third monkeys, the electrical marking were made at the last recording session and the sections of the brain were stained with a modified silver stain for myelinated fibers (Gallyas 1979). The positions of electrical marking were located at the densely myelinated zone (DMZ) at the anterior bank of the superior temporal sulcus (Fig. 4) and this confirmed that the recording was made from MSTd (Komatsu and Wurtz 1988).

RESULTS

I recorded from 114 MSTd neurons that responded significantly (t test; $p < 0.05$) to at least one stimulus in the basic stimulus set. Next, I examined the responses of these neurons to the plane stimulus set. Ninety-seven of these exhibited significant responses to at least one of the plane stimulus set that were more than half of the maximum response to the basic stimulus set. Further analysis of the responses to the plane stimulus set was conducted for these 97 neurons.

Responses to the basic stimulus set

First, I tested responses to the basic stimulus set to examine selectivity to the basic optic flow patterns, which has been employed in past studies in MSTd and has been shown to characterize MSTd neurons. Fig. 6 shows one example of the neurons that responded selectively to the basic stimulus set. This neuron showed the maximum response to the clockwise rotation and also responded to the expansion. The relationship between the responses to the basic stimulus set and the responses to the plane stimulus set will be mentioned later. Neurons that significantly responded to at least one of the stimuli in the basic stimulus set was used for further test using plane stimuli.

Responses to the plane stimulus set

To examine whether MSTd neurons could code a 3D-orientation of the rotating plane, I tested responses to the plane stimulus set and analyzed the selectivity to tilt and slant.

Fig. 7A shows the responses to the plane stimulus set of the same neuron in Fig. 6.

This neuron responded selectively to the plane stimulus set. The responses of this neuron increased as slant increased while the tilt was kept constant at 135°. On the contrary, with the constant tilt of 45°, the responses decreased as slant increased. Apparently, the responses of this neuron to the plane stimulus set changed depending on both tilt and slant. The bubble plots of the same responses are shown in Fig. 7B. Again, the large responses were obtained for the stimuli with 0° and 135° of tilt and with steeper slants. Due to the orthographic projection, the stimuli with 180° of tilt and those with 0° of tilt are indistinguishable. Hence the preferred tilt of this neuron is between 135° and 180° of tilt (or between -45° and 0° of tilt). Other examples of the neurons that responded selectively to both tilt and slant are shown in Fig. 13.

Figure 8 shows two examples of the neurons that had different types of selectivity to the plane stimulus set. The neuron in Fig. 8A responded maximally to the stimulus with 90° of tilt and 40° of slant. It responded well to the stimuli with 45° and 90° of tilt, but slant did not clearly affect the responses. Another neuron, shown in Fig. 8B, responded well to the stimuli with shallower slants, irrespective of tilt. The maximum response was to the stimulus with 0° of tilt and 20° of slant.

Quantification of selectivity

To examine how the neurons that were selective to tilt and/or slant represent the 3D-orientation of the rotating plane, I analyzed selectivity quantitatively as described in METHODS. To test the significance of tilt and slant selectivity, I examined the variations of two sets of responses to the stimuli that shared the same slant and tilt with the best stimulus (ANOVA, $p < 0.05$). Figure 9 plots the same responses as shown in Fig. 7 as a function of tilt (Fig. 9A) and slant (Fig. 9B). The best stimulus in Fig. 9 is

the one with 135° of tilt and 60° of slant. So, the significance of tilt and slant selectivity was examined using the responses as indicated by solid symbols in Fig. 9, A and B, respectively. This neuron showed significant selectivity to both tilt and slant. To quantify the selectivity, I also computed a selectivity index for tilt and slant using the same two sets of responses. For these responses, the selectivity index for tilt was 0.94, and that for slant was 0.60.

Figure 10 shows the scatter diagram of the selectivity indices of the 97 neurons that responded significantly to the plane stimulus set. The presence or absence of selectivity (in light of the above criteria) to tilt and/or slant is also indicated by different symbols. The selectivity index distributed continuously and, with respect to the degree of selectivity, there is no distinguishable cluster of neurons. Of the neurons that responded significantly to the plane stimulus set, many neurons (65/97, 67%) exhibited selectivity to at least either tilt or slant. Of these, 17 were selective only to tilt, 23 only to slant, and 25 to both.

The distributions of preferred tilt and slant are shown in Fig. 11. In the distribution of preferred tilt, there is a significant bias to 90° (Rayleigh test, $p = 0.014$). In the distribution of preferred slant, there are two peaks at 20° and 60°. Neurons with different slant selectivity had different tilt selectivity. The solid bars represent neurons selective to both tilt and slant, whereas the open bars represent neurons selective only to tilt (A) or slant (B). Almost all neurons preferring the steeper slant were also selective to tilt, whereas those preferring the shallower slant were not selective to tilt. This result seems reasonable when considering the distances between stimuli in the tilt-slant space (Fig. 2C). That is, the distance between two stimuli with steeper slants is larger compared with the distance between two stimuli with shallower slants even if the tilt

difference is held constant. This may result in a larger difference in the responses to two stimuli differing by the same amount of tilt when the slant is steeper, but a smaller difference in the responses when the slant is shallower.

Selectivity to the basic and plane stimulus set

Area MSTd has been characterized by the presence of neurons that are selective to optic flow patterns similar to the stimuli in the basic stimulus set (Duffy and Wurtz 1991; Lagae et al. 1994; Saito et al. 1986; Tanaka and Saito 1989). Thus it would be important to know how the neurons examined in the present study respond to such optic flow stimuli. The relationships between the selectivity to the basic stimulus set and selectivity to the plane stimulus set is summarized in Fig. 12. The stimuli in the basic stimulus set can be classified into three stimulus classes (Duffy and Wurtz 1991): planar (four translations), radial (expansion and contraction), and circular (two rotations). As was shown previously (Duffy and Wurtz 1991; Graziano et al. 1994; Lagae et al. 1994), some MSTd neurons responded to only one stimulus class, but some others responded to more than one stimulus class. I classified neurons according to the number of stimulus classes in the basic stimulus set that evoked responses greater than half of the maximum response. Neurons that responded to only one class were classified as single-component, those that responded to two classes were classified as double-component, and those that responded to three classes as triple-component. Of the 97 neurons examined, 42 neurons were classified as single-component, 30 as double-component, and 25 as triple-component.

There existed relationships between the selectivity to the basic stimulus set and to the plane stimulus set in two respects. The first one was between the neurons that

responded to the circular motion stimuli in the basic stimulus set and the neurons preferring shallower-slant stimuli. The rotating plane stimuli employed in the present study obviously include rotation as an element of the stimulus. This is particularly clear for stimuli with shallower slants such as 0° and 20° which are nearly identical to the circular motion stimuli in the basic stimulus set. Thus I can expect that neurons responsive to the stimuli with shallower slants would be sensitive to the circular motion stimulus in the basic stimulus set. Actually, out of 21 neurons preferring the stimuli with 0° or 20° of slant, 19 neurons responded maximally to the circular motion stimuli in the basic stimulus set. Another relationship was that most of the neurons preferring the stimuli with steeper slants such as 60°, most of which were also selective to tilt (Fig. 11), were classified as double- or triple-component (Fig. 12). No other clear relationship was found between the selectivity to the basic stimulus set and that to the plane stimulus set.

Responses to the non-preferred rotation

One conspicuous feature of the rotation sensitive neurons in area MSTd is their selectivity to the direction of rotation (Saito et al. 1986). As the 3D surface orientation of the rotating plane employed in the present study is defined independently of the direction of rotation, each plane with a particular combination of tilt and slant could rotate either clockwise or anticlockwise. Therefore it is of interest to know whether neurons selective to tilt and/or slant of the rotating plane are also selective to the direction of rotation. For 48 neurons selective to either tilt or slant, I compared the responses to the plane stimuli in the preferred direction of rotation (preferred rotation) and the opposite direction of rotation (non-preferred rotation). Figure 13 shows three

examples of such neurons. The neuron in Fig. 13A responded well to the anticlockwise rotating stimuli and exhibited selectivity to both tilt and slant (preferred rotation, left panel). This neuron did not show any clear response to clockwise rotating stimuli (non-preferred rotation, right panel). Likewise, of the neurons tested in both directions of rotation, 24 neurons (24/48, 50%) showed rotation-direction selective responses in which the best response in the preferred rotation was more than twice as strong as that in the non-preferred rotation. Among the remaining neurons, some responded equally in both directions of rotation (Fig. 13B). However, most neurons, when tested in the non-preferred rotation, responded only to a sub-set of the stimuli that caused responses when tested in the preferred rotation. An example of such responses is shown in Fig. 13C.

To compare the overall responsiveness in the preferred rotation direction with that in the non-preferred rotation direction, all the responses to the stimuli in the plane stimulus set for each rotation were summed, and the sum for the non-preferred rotation was divided by the sum for the preferred rotation. In 33 out of the 48 neurons tested (69%), the computed ratio was less than 0.5. Thus a majority of neurons had selectivity not only to tilt and/or slant of the plane stimuli, but also to the direction of rotation of the plane stimuli.

I then compared the optimal slant and tilt of the plane stimuli between different rotations for 24 neurons in which the best response of all the non-preferred rotation stimuli was more than half of the best response to all the preferred rotation stimuli. Figure 14 shows distributions of the differences in the optimum tilt and slant of these 24 neurons. All these neurons had selectivity to either tilt or slant in the preferred rotation. Neurons that also exhibited selectivity to tilt or slant to the stimuli in the non-preferred

rotation are shown with filled bars. Both the distributions of the differences in the optimum tilt and slant had peaks at 0°. Thus many neurons responded maximally to the stimuli with the same tilt and slant between the preferred and the non-preferred rotations.

These results indicate that many MSTd neurons that are selective to tilt and/or slant of the plane stimuli also exhibit selectivity to the direction of rotation, at least to some extent, but some neurons may encode tilt and/or slant independent of the direction of rotation.

Position invariance

Is the selectivity I observed really for tilt and/or slant? With the change in the tilt and/or slant, other stimulus elements in the plane stimuli also change (Fig. 15). The direction of local translational motion is one such stimulus element and if the neuron tested is a detector of translational motion direction, it may also show an apparent selectivity to tilt and/or slant. To examine the possibility that the neurons responded not to the entire stimulus pattern, but merely responded to the direction of local translational motion, position invariance was tested. At five positions within the RF, the best stimulus in the plane stimulus set and a stimulus with the same slant and tilt as the best stimulus but with the opposite direction of rotation was presented. Of these five positions, one was at the center of the RF and the remaining four positions were at the peripheries within the RF (Fig. 16A). I tested the position invariance for 24 neurons, which exhibited a significant difference (t test, $p < 0.05$) in the responses to the stimuli in different directions of rotation at the central position. Out of 24 neurons tested, one neuron was selective only to tilt, 11 only to slant, and 12 to both. When the

stimulus is moved to the peripheral position, the direction of local translational motion is reversed even though the entire stimuli are rotating in the same direction (Fig. 16A). If the neurons are responding to the direction of local translational motion, the relative magnitude of the response between two directions of rotation should change depending on its stimulus position. Figure 16B shows an example of the results of this test for one neuron. The responses to the preferred rotation were significantly stronger than those to the non-preferred rotation at every position tested. Such position invariance was observed in most neurons. To evaluate the degree of position invariance, I calculated a position invariance index for each neuron (Graziano et al. 1994). . First, I calculated the direction selectivity index at each of the five positions as 1 – (response to the non-preferred rotation) / (response to the preferred rotation). Note that "preferred rotation" means the direction of rotation the cell prefers when presented at the central position and, hence, the index could go negative in the periphery if the cell shows the opposite preference there. Then, a position invariance index was computed by dividing the direction selectivity index obtained at each peripheral position by that obtained at the central position. Thus, four position invariance indices were calculated for each neuron. If the preferred direction of rotation was the same at the central and peripheral positions, the position invariance index is positive. If the direction selectivity indices are equivalent, then the ratio is unity. Finally, if the preferred direction of rotation changes, then the position invariance index is negative.

The distribution of 93 position invariance indices for 24 neurons exhibited a peak at unity and almost all had positive values (Fig. 16C). (Of a total of 96 responses, four responses to peripheral stimuli in each of 24 neurons, three responses of three neurons were excluded from the analysis because no clear responses were obtained to both the

preferred and non-preferred rotations in these case. In these cases, the stimuli might have been laid outside the RF.) Seventy-six out of 93 position invariance indices were between 0.5 and 1.5. These results indicate that the selectivity to the direction of rotation did not change significantly within the RF. Thus, the results suggest that the selectivity to tilt and/or slant of the plane stimuli was not due to the direction of local translational motion.

Rotation speed

Another stimulus element that changed together with the change in the tilt and/or slant of the plane stimuli is the speed of the motion. It has been shown that some MST neurons are sensitive to stimulus speed (Duffy and Wurtz 1997; Orban et al. 1995). Since I employed an aperture for the plane stimuli, the maximum speed in the stimuli changed with the change of slant (Fig. 17A). Thus the slant selectivity I observed might reflect sensitivity to local speed. To examine this possibility, I investigated the selectivity to slant of the stimuli with three different rotation speeds for 29 slant selective neurons (Fig. 17B). Note that local speed gradients in the plane stimuli, which itself may cause depth perception (Braunstein 1968; Harris et al. 1992), also changed with the change in rotation speed. For example, speed gradients along the direction of tilt, which contained the maximum speed and thus contained the maximum magnitude of the speed gradient, also changed with the change in rotation speed. Thus, in this control experiment, the effects of both local speed and local speed gradients were examined.

The effect of speed was statistically evaluated by two-way ANOVA with slant and speed as the main factors. Of 29 neurons examined, the rotation speed had no

significant effect on 21 neurons ($p > 0.01$). One example of such neurons is shown in Fig. 18A. In the left column, the responses are plotted against slant. The data showed a very good agreement across rotation speeds, despite the fact that local speeds and speed gradients contained in the stimuli at these three rotation speeds are quite different. In the right column, the set of responses is replotted against the maximum speed in the stimulus. If this neuron was responding to speed, the degree of response overlap should be greater when the responses were sorted according to speed. However, this was clearly not the case and the degree of response overlap was much more prominent when the responses were sorted according to slant. Seven of the remaining neurons showed a significant effect ($p < 0.01$) of the rotation speed. One of such neurons is shown in Fig. 18B. This neuron exhibited stronger responses to steeper-slant stimuli regardless of rotation speed. Because the maximum speed in the stimulus was larger for steeper-slant stimuli, there was the possibility that this neuron might be more sensitive to stimuli with faster speeds. However, this was not the case because this neuron responded more strongly to more slowly rotating stimuli than to faster rotating stimuli. Like this example, in five of these seven neurons, the sensitivity to slant was not simply explained by the sensitivity to the rotation speed. Two other neurons exhibited response changes that were consistent with the prediction from their slant selectivity. These neurons exhibited stronger responses to steeper-slant stimuli and responded more strongly to stimuli rotating faster. The slant selectivity of these neurons may be explained by the sensitivity to local speed or speed gradient. Only one neuron exhibited significant interaction between slant and rotation speed. Taken together, I concluded that, for nearly all neurons examined, the slant selectivity cannot be attributed to local speed or local speed gradients in the stimuli.

Shuffled plane stimulus

Finally, I examined whether the recorded neurons were really sensitive to the structure of the velocity field in the stimulus. Each plane stimulus has a specific distribution of velocities. Thus, if the neurons simply responded to the distribution of velocities regardless of their spatial configuration, the neurons would show apparent selectivity to tilt and slant. To examine this possibility, I recorded the responses of 15 neurons, which exhibited selectivity to tilt and/or slant, to the stimuli whose locations of dots were shuffled while preserving their velocities (shuffled stimuli, see Methods and Fig. 19). These stimuli do not contain 3D information and are not perceived as 3D plane although the distribution of velocities is the same as the original plane stimulus.

Fig. 19 shows responses of a neuron to the plane stimuli (left column) and the shuffled stimuli (right column). This neuron clearly responded to the plane stimulus set and exhibited tilt selectivity. However, this neuron did not exhibit significance response to any of the stimuli in the shuffled stimulus set. Similarly, most of the neurons tested showed much weaker responses to the shuffled stimuli compared with the plane stimuli. In 13 out of 15 neurons tested, the maximum response to the shuffled stimuli was significantly weaker than that to the plane stimuli ($p < 0.05$, t test), and in 10 of these, the relative magnitude of the response was less than 0.5. These results indicate that the sensitivity to slant and/or tilt of the recorded neurons cannot be attributed to mere sensitivity to the velocity distributions. I concluded that these neurons were responding to the overall structure of the velocity field of the stimuli.

DISCUSSION

To examine the role of area MSTd in SFM processing, I assessed the selectivity of MSTd neurons to the 2D visual stimuli that simulated 3D-oriented rotating planes. Two-thirds of the neurons that responded to these stimuli had selectivity for at least one of the stimulus parameters, namely tilt and/or slant, that can define the simulated 3D surface orientation of the rotating plane. This selectivity could not be attributed to the direction of local translational motion, local speed, local speed gradients or distribution of velocities in the stimuli. The preferred tilt and slant of MSTd neurons were distributed across the whole range of the stimuli used (Fig. 11). Thus, area MSTd can code the 3D surface orientation and these results suggest that area MSTd is involved in SFM processing.

How does area MSTd represent surface orientation?

I showed that MSTd neurons have selectivity to tilt and/or slant of rotating planes. How, then, do these neurons represent the surface orientation in area MSTd? The selectivity to slant and tilt varied among MSTd neurons. Some neurons were selective to steeper slants with tilt selectivity, some others were selective to shallower slants without tilt selectivity, and still others were selective only to tilt. To represent the whole range of slant, it should be necessary to sum the signals from neurons with different preferred slants with various weights. The tilt of the stimulus may be represented by the activities of tilt sensitive neurons.

Seyama et al. (2000) reported a psychophysical study employing stimuli similar to those used in the present study. They found that the visual stimulation by the rotating

random dot plane caused a slant after-effect, and that this slant after-effect had a tilt dependency. They suggested that the processing of tilt and slant are not independent in humans and proposed that two types of detectors, tilt-sensitive slant detectors and tilt detectors, may be involved in surface orientation processing. The first type of detector in the model may correspond to the weighted summation of the signals from the neurons selective to tilt as well as to slant and those selective only to slant, and the second type of detector may correspond to neurons selective to tilt.

Elements in the rotating plane for recovery of 3D structure

Numerous stimulus elements vary with the change in the orientation of the rotating plane; namely, local translational motion, local speed, local speed gradients, distribution of velocities, shearing motion, and orbit of the moving dot. In these elements listed, local translational motion, local speed and distribution of velocities in the stimulus do not correlate to the simulated 3D-orientation. The control experiments showed that the selectivity to the plane stimuli could not be attributed merely to the selectivity to these elements in the stimuli.

The speed gradients in the plane stimuli also do not correlate to the simulated 3D-orientation. Psychophysical studies, however, have demonstrated that humans can perceive depth from the speed gradients, meaning that the speed gradient is an important clue for recovering the 3D structure from the 2D image (Braunstein 1968; Harris et al. 1992). Some electrophysiological studies demonstrated that MT neurons are sensitive to the speed gradients in planar motion (Treue and Andersen 1996; Xiao et al. 1997). Thus it is possible that the MSTd neurons I examined in the present study receive signals of local speed gradients in the plane stimuli from area MT. However, the

control experiment employing various rotation speeds suggests that the slant selectivity cannot be explained by local speed gradients in the stimuli. In this control experiment, although local speed gradients changed together with the change in rotation speed, the slant selectivity did not change in a manner consistent with that of local speed gradients. Thus, the speed gradients in the plane stimuli themselves do not correspond to the simulated 3D-orientation and also do not contribute to the formation of selectivity to the plane stimuli of MSTd neurons.

What kind of elements, then, contributes to the formation of plane selectivity? One possible candidate is the integration of speed gradients. In the rotating plane stimuli, the magnitude of the speed gradient along the direction of tilt is maximal and that along the direction orthogonal to it is minimal. The ratio between these two values uniquely corresponds to the slant and is invariant with the change in the speed of the stimulus. Signals about the local speed gradient extracted in area MT, thus, may be compared across different regions in the plane stimuli in area MSTd to compute the surface orientation in a manner independent of the local speed of the moving dots (Fig. 20).

Another possible candidate is the pattern of the orbit of each moving dot in the plane stimuli. This also provides a clue to recover the 3D-orientation of the rotating plane. Although each dot in the stimuli had limited lifetime so that each dot did not establish the complete elliptic orbit, MSTd neurons might exploit the information about orbit curvature if they could interpolate the orbits of the moving dots across time and space. Psychophysical experiments have suggested that space-time interpolation of motion of dots with limited lifetimes occurs in the processing of SFM perception (Treue et al. 1991). Sakata et al. (1994) found that neurons in the superior temporal sulcus (STS) near area MSTd had selectivity to the rotation-in-depth of single dots. These STS

neurons seem to have information about orbit. Thus, it may be possible that MSTd neurons also exploit information about the orbit of the moving dots, although MSTd neurons do not respond well to the motion of a single dot.

Cue invariant representation of surface orientation

Area MSTd is believed to be involved in higher motion processing. Sensitivity of MSTd neurons recorded in the present study to the direction of rotation as well as to the simulated 3D-orientation of the rotating plane suggests that these neurons specifically encode surface orientation defined by motion cues. A question arises whether surface orientation is represented in a cue-invariant manner in some other cortical areas. An fMRI study about 3D motion found activation of many areas in the intraparietal sulcus (IPS) in addition to MT+, the putative homologue of areas MT and MST in the macaque (Orban et al. 1999). In the macaque, neurons in the caudal area in the intraparietal sulcus (CIP) are shown to have selectivity to a surface orientation defined by disparity as well as texture gradients (Taira et al. 2000; Tsutsui et al. 1999). This result suggests that information about surface orientation defined by different cues such as disparity and texture gradients are integrated in CIP. MSTd neurons project to this area (Boussaoud et al. 1990). Although it is unknown whether CIP neurons are also selective to a surface orientation defined by motion, there is a possibility that the surface orientation extracted from motion information may reach CIP and that CIP neurons represent surface orientation in a visual cue-independent manner.

Optic flow

Theoretically, optic flow can be decomposed into four elements; translation,

expansion / contraction, rotation, and deformation; of these, only deformation provides information about the structure of the environment in a manner independent from the self-motion (Koenderink 1986). Thus selectivity to deformation might be related to the encoding of the structure of the environment. Because few MSTd neurons exhibited selectivity to deformation stimuli, Lagae et al. (1994) concluded that area MSTd is not involved in the processing of SFM. However, MSTd neurons were selective to the combination of these four elements and thus optic flow may not be decomposed into these elements in area MSTd (Graziano et al. 1994; Paolini et al. 2000). Thus the lack of selectivity to deformation does not necessarily mean that area MSTd is not involved in the processing of SFM. Indeed, some MSTd neurons were selective to axial expansion / contraction, which can be described as the combination of expansion / contraction and deformation, and others were selective to shear stimuli, which can be described as the combination of rotation and deformation (Tanaka et al. 1989). The plane stimulus set employed in the present study is also made of combinations of rotation and deformation in various ratios. Thus, MSTd neurons may not encode deformation by itself; instead, they may encode the combination of deformation and the other elements of optic flow.

In the present study, I showed that MSTd neurons have selectivity to rotating planes and suggested an involvement of area MSTd in the processing of SFM. But those neurons exhibiting selective responses to the rotating plane also had selectivity to the basic stimulus set or basic optic flow patterns. Selective responses of MSTd neurons to optic flow stimuli have often been interpreted in relation to the sensitivity to self-motion (Britten and van Wezel 1998; Duffy and Wurtz 1991; Lagae et al. 1994; Lappe et al. 1993; Lappe and Rauschecker, 1996; Perrone and Stone 1994; Saito et al. 1986;

Tanaka and Saito 1989). However, SFM is a phenomenon of recovering the structure of objects from motion. Does this mean that the neurons recorded in the present experiment are related to both self-motion and object-motion? Since motion patterns similar to optic flow can be generated by object-motion, selectivity to the optic flow does not necessarily indicate of relation to the self-motion. Some reports suggested that MSTd neurons that were selective to optic flow may be related to the processing of the object-motion (Geesaman and Andersen 1996; Graziano et al. 1994). Thus it is possible that the neurons with selectivity for optic flow, and selectivity for rotating planes, may be solely involved in the processing of object-motion.

However, there still is a possibility that part of the selectivity for plane stimuli is due to the coding of self-motion. The shearing motion contained in the plane stimuli is reminiscent of the motion parallax generated by self-motion. A significance bias to 90° in the preferred tilt distribution (Fig. 11A) might be related to the motion parallax caused by ground surfaces during self-motion. How processing of self-motion and object-motion are separated, or overlapped, in area MSTd is still an open question and needs further experimentation.

ACKNOWLEDGEMENTS

I am very grateful to Professor Hidehiko Komatsu for his supervising my study. I thank my collaborators, Dr. Ikuya Murakami, Dr. Krishna V. Shenoy and Professor Richard A. Andersen for their kind helps and their contribution to my study. I also thank I. Yokoi for myelin staining. I also thank M. Togawa, M. Yoshitomo, and N. Takahashi for technical assistance. Professors Tadashi Isa, Shigemi Mori, Yoshiki Kaneoke, and Akichika Mikami judged my doctoral degree and gave me a helpful comments. People in my laboratory, Professor Minami Ito, Dr. Akitoshi Hanazawa, Dr. Tadashi Ogawa, Dr. Masaharu Kinoshita, Dr. Kowa Koida, Dr. Hideki Kondo, Toshiki Tani, Masayuki Matsumoto, Yuka Nakane, Miki Tsuzuki, and Tomoko Fujii, also helped my study in every aspects. People in the National Institute for Physiological Sciences and the Graduate University for Advanced Studies also kindly helped me.

Finally, I have to thank my family, my friends, and my wife, Takako.

REFERENCES

Andersen RA, Bradley DC, and Shenoy KV. Neural mechanisms for heading and structure from motion perception. *Cold Spring Harbor Symp Quant Biol* 61:15-25, 1996.

Boussaoud D, Ungerleider LG, and Desimone R. Pathways for motion analysis: cortical connections of the medial superior temporal and fundus of the superior temporal visual areas in the macaque. *J Comp Neurol* 296: 462-495, 1990.

Bradley DC, Chang GC, and Andersen RA. Encoding of three-dimensional structure-from-motion by primate area MT neurons. *Nature* 392: 714-717, 1998.

Braunstein ML. Motion and texture as sources of slant information. *J Exp Psychol* 78: 247-253, 1968.

Britten KH and van Wezel RJA. Electrical microstimulation of cortical area MST biases heading perception in monkeys. *Nature Neurosci* 1: 59-63, 1998.

Duffy CJ and Wurtz RH. Sensitivity of MST neurons to optic flow stimuli. I. A continuum of response selectivity to large-filed stimuli. *J Neurophysiol* 65: 1329-1345, 1991.

Duffy CJ and Wurtz RH. Medial superior temporal area neurons respond to speed patterns in optic flow. *J Neurosci* 17: 2839-2851, 1997.

Gallyas F. Silver staining of myelin by means of physical development. *Neurol Res* 1: 203-209, 1979.

Geesaman BJ and Andersen RA. The analysis of complex motion patterns by form/cue invariant MSTd neurons. *J Neurosci* 16: 4716-4732, 1996.

Graziano MSA, Andersen RA, and Snowden RJ. Tuning of MST neurons to spiral

motions. *J Neurosci* 14: 54-67, 1994.

Harris M, Freeman T, and Hughes J. Retinal speed gradients and the perception of surface slant. *Vision Res* 32: 587-590, 1992.

Hildreth EC, Ando H, Andersen RA, and Treue S. Recovering three-dimensional structure from motion with surface reconstruction. *Vision Res* 35: 117-137, 1995.

Koenderink JJ. Optic flow. *Vision Res* 26: 161-180, 1986.

Komatsu H and Wurtz RH. Relation of cortical areas MT and MST to pursuit eye movements. I. Localization and visual properties of neurons. *J Neurophysiol* 60: 580-603, 1988.

Lagae L, Maes S, Raiguel S, Xiao DK, and Orban GA. Responses of macaque STS neurons to optic flow components: a comparison of areas MT and MST. *J Neurophysiol* 71: 1597-1626, 1994.

Lappe M, Bremmer F, Pekel M, Thiele A, and Hoffman KP. Optic flow processing in monkey STS: a theoretical and experimental approach. *J Neurosci* 16: 6265-6285, 1996.

Lappe M and Rauschecker JP. A neural network for the processing of optic flow from ego-motion in man and higher mammals. *Neural Comput* 5: 374-391, 1993.

Maunsell JHR and Van Essen DC. The connections of the middle temporal visual area (MT) and their relationship to a cortical hierarchy in the macaque monkey. *J Neurosci* 3: 2563-2586, 1983.

Orban GA, Lagae L, Raiguel S, Xiao D, and Maes H. The speed tuning of medial superior temporal (MST) cell responses to optic-flow components. *Perception* 24: 269-285, 1995.

Orban GA, Sunaert S, Todd JT, Van Hecke P, and Marchal G. Human cortical regions

involved in extracting depth from motion. *Neuron* 24: 929-940, 1999.

Paolini M, Distler C, Bremmer F, Lappe M, and Hoffman KP. Responses to continuously changing optic flow in area MST. *J Neurophysiol* 84: 730-743, 2000.

Perrone JA and Stone LS. A model of self-motion estimation within primate extrastriate visual cortex. *Vision Res* 34: 2917-2938, 1994.

Qian N and Andersen RA. Transparent motion perception as detection of unbalanced motion signals. II. Physiology. *J Neurosci* 14: 7367-80, 1994.

Raiguel S, Van Hulle MM, Xiao DK, Marcar VL, Lagae L, and Orban GA. Size and shape of receptive fields in the medial superior temporal area (MST) of the macaque. *NeuroReport* 8: 2803-2808, 1997.

Robinson DA. A method of measuring eye movement using a scleral search coil in a magnetic field. *IEEE Trans Biomed Eng* 10: 137-145, 1963.

Saito H, Yukie M, Tanaka K, Hikosaka K, Fukada Y, and Iwai E. Integration of direction signals of image motion in the superior temporal sulcus of the macaque monkey. *J Neurosci* 6: 145-157, 1986.

Sakata H, Shibutani H, Ito Y, Tsurugai K, Mine S, and Kusunoki M. Functional properties of rotation-sensitive neurons in the posterior parietal association cortex of the monkey. *Exp Brain Res* 101: 183-202, 1994.

Seyama J, Takeuchi T, and Sato T. Tilt dependency of slant aftereffect. *Vision Res* 40: 349-357, 2000.

Siegel RM and Andersen RA. Perception of three-dimensional structure from motion in monkey and man. *Nature* 331: 259-261, 1988.

Sugihara H, Murakami I, Komatsu H, Shenoy KV, and Andersen RA. Selectivity of neurons to the 3D orientation of a rotating plane in area MSTd of the monkey. *Soc*

Neurosci Abstr 24: 649, 1998.

Taira M, Tsutsui K, Jiang M, Yara K, and Sakata, H. Parietal neurons represent surface orientation from the gradient of binocular disparity. *J Neurophysiol* 83: 3140-3146, 2000.

Tanaka K, Fukada Y, and Saito H. Underlying mechanisms of the response specificity of expansion/contraction and rotation cells in the dorsal part of the medial superior temporal area of the macaque monkey. *J Neurophysiol* 62: 642-656, 1989.

Tanaka K and Saito H. Analysis of motion of the visual field by direction, expansion/contraction, and rotation cells clustered in the dorsal part of the medial superior temporal area of the macaque monkey. *J Neurophysiol 62*: 626-641, 1989.

Treue S and Andersen RA. Neural responses to velocity gradients in macaque cortical area MT. *Vis Neurosci* 13: 797-804, 1996.

Treue S, Husain M, and Andersen RA. Human perception of structure from motion. *Vision Res* 31: 59-75, 1991.

Tsutsui K, Taira M, Min J, and Sakata H. Coding of surface orientation by the gradient of texture and disparity in the monkey caudal intraparietal area. *Soc Neurosci Abstr* 25: 670, 1999.

Ullman S. The interpretation of structure-from-motion. *Proc R Soc Lond B Biol Sci* 203: 405-426, 1979.

Ungerleider LG and Mishkin M. *Two cortical visual systems.* In: Ingle DJ, Goodale MA, and Mansfield RJW (eds). *Analysis of Visual Behavior.* Cambridge: MIT Press, 1982, p. 549-586.

Ungerleider LG and Desimone R. Cortical connections of visual area MT in the macaque. *J Comp Neurol* 248: 190-222, 1986.

Wallach H and O'Connell DH. The kinetic depth effect. *J Exp Psychol 45*, 205-217, 1953.

Xiao DK, Marcar VL, Raiguel SE, and Orban GA. Selectivity of macaque MT/V5 neurons for surface orientation in depth specified by motion. *Eur J Neurosci* 9: 956-964, 1997.

LEGENDS

Fig. 1. The dorsal pathway. This schema shows the dorsal pathway, which is involved in processing of motion information. The left schema shows a side view of the monkey cerebral cortex (left for anterior, right for posterior), highlighting areas composing the dorsal pathway; V1, MT and MST. The superior temporal sulcus (STS) is opened to show the inside. The right schema shows examples of motion stimuli that neurons in each area preferably respond.

Fig. 2. The plane stimulus set. *A*: Schematic illustration of the rotating plane stimulus. The plane stimulus was composed of random dots and simulated a rotating plane with a particular 3D-orientation (left). Small solid squares indicate moving random dots. The pattern is rotated about the surface normal vector passing through the center. The direction of rotation in this figure is anticlockwise and is indicated by arrows. Positions of the dots are calculated by using orthographic projection to remove perspective information. The unshaded circle within the shaded rectangle illustrates the aperture I employed for the plane stimulus set to avoid a change in the spatial extent of the stimulus pattern accompanying with the change in simulated 3D-orientation. Only the unshaded part is presented as a visual stimulus. The right illustration depicts a plane stimulus used in this experiment with arrows indicating speed of moving dots by their length. *B*: Tilt and slant. A simulated 3D-orientation is defined by two parameters, namely, tilt and slant. The slant is the angle that indicates how much a plane orients. The tilt is the angle that indicates which direction a plane orients. *C*: Schematic illustration of plane stimuli with different simulated 3D-

orientations. Each ellipse indicates a stimulus and is plotted in the tilt-slant space at the location corresponding to its simulated 3D-orientation. The shape of the ellipse indicates schematically the simulated 3D-orientation of the stimulus although actual spatial extents of the stimuli are the same because of the aperture. I used a set of four tilts, namely, 0°, 45°, 90°, and 135°, and a set of four slants, namely, 0°, 20°, 40°, and 60°. At 0° slant, the stimulus is on the frontoparallel plane and tilt cannot be defined. The plane stimulus set consists of the combination of each tilt and slant, thus, a total of 13 stimuli (4 tilts × 3 slants + 0°-slant stimulus) are in this set. Because of the orthographic projection, the stimuli have an ambiguity with respect to tilt such that two stimuli having the tilt difference of 180° are identical to each other. Such identical pairs of stimuli are illustrated in black and gray, respectively.

Fig. 3. The experimental equipment. Each monkey sat in a primate chair and looked at the CRT display binocularly. Neural activities were amplified, discriminated and converted to pulse sequences. Eye position was monitored with an eye coil. Computer controlled data collection, events for the fixation task, and stimulus presentation.

Fig. 4. The fixation task. The fixation task was initiated with appearance of a fixation point (FP) on the CRT display. The visual stimulus was turned on 500 ms after the monkey foveated the FP and was presented for 1000 ms. The top row schematically illustrates the CRT display. The middle and bottom rows indicate time courses of the stimulus and the fixation point, respectively.

Fig. 5. The Recording sites. Bottom; Schematic illustration of a side view of the monkey cerebral cortex (left for posterior, right for anterior). The superior temporal sulcus (STS) is opened to show the inside. The approximate location of MST was indicated by filled region. Top; The photomicrograph of the myelin stained parasagittal section at the site indicated by the horizontal line in the bottom schema. Two arrows indicate the electrical markings. DMZ; Densely myelinated zone.

Fig. 6. Responses of a neuron to the basic stimulus set. Each peristimulus time histogram and raster indicates the responses of a neuron to the four trials of the corresponding stimulus. Schematic illustrations of the stimuli are presented above the histograms and the rasters. Short vertical lines on the raster display indicate cell discharges; successive lines represent successive trials. The rasters and histograms are aligned at the stimulus onset (vertical line). The vertical calibration line on the left of each histogram indicates 100 spikes/s. The horizontal line below each histogram indicates the period of stimulus presentation (1 s). This neuron maximally responded to the clockwise rotation and also responded to the expansion.

Fig. 7. Responses of an example neuron selective to both tilt and slant of the rotating plane stimulus set. This neuron is the same neuron as shown in Fig. 6. *A*: Each peristimulus time histogram indicates the responses of a neuron to a stimulus with certain tilt and slant. The histogram is placed at a position representing each stimulus in the tilt-slant space. Other conventions are as in Fig. 6. *B*: The same responses shown in *A* are replotted as a bubble plot. The diameter of the circle represents the response amplitude. The scale is at the bottom left. The mirror image of the

responses is also shown in gray. The arrow at the bottom right indicates the direction of rotation of the stimuli (in this case, clockwise).

Fig. 8. Two examples of neurons exhibiting different types of selectivity to the plane stimulus set. *A*: A neuron responding well to the stimuli with 45° and 90° of tilt. Slant did not clearly affect the responses. *B*: A neuron responding well to the stimuli with shallower slants irrespective of tilt. Conventions are as in Fig. 7B.

Fig. 9. Replot of the responses of the neuron as shown in Fig. 7 as a function of tilt (A) and slant (B). The abscissa indicates tilt (A) and slant (B) and the ordinates indicate the amplitude of the response. Different symbols represent the responses to the stimuli with different slants (A) and tilts (B). "X" in *B* indicates the response to the stimulus with 0° of slant. Error bars are standard deviations. The largest response was obtained when tilt was 135° and slant was 60° (best stimulus). Solid squares indicate the responses to the stimuli that share the same slant (A) and tilt (B) with the best stimulus. I calculated the selectivity indices for tilt (A) and slant (B) from these responses. The selectivity index of this neuron was 0.94 for tilt and 0.60 for slant and was significantly tuned for tilt and slant by one-way ANOVA ($p < 0.05$).

Fig. 10. Distribution of the selectivity indices. The bottom left panel shows the scatter diagram of the selectivity indices of 97 neurons that responded significantly to the plane stimulus set. Each symbol represents a neuron and different symbols indicate the presence or absence of the selectivity to tilt and/or slant as shown in the inset (one-way ANOVA, $p < 0.05$). The top and right panels show the distribution of

the selectivity index for tilt and slant, respectively. Filled bars in each histogram indicate the neurons that exhibited significant responses, and open bars indicate those that did not.

Fig. 11. Distributions of the preferred tilt (A) and slant (B). The abscissa indicates tilt (A) and slant (B) that induced the maximum response, and the ordinates indicate the number of neurons. Only the neurons that were selective to either tilt (A) or slant (B) contributed to these histograms. Filled bars represent, in total, 25 neurons selective to both tilt and slant, and open bars represent neurons selective only to tilt (A) or slant (B). In *A*, a significant bias to 90° is observed (Rayleigh test, $p = 0.014$). In *B*, there are two peaks at 20° and 60° in the preferred slant distribution. See the text for more details.

Fig. 12. Relationship between the selectivity to the basic stimulus set and to the plane stimulus set. Different columns indicate the selectivity to tilt and/or slant of the plane stimulus set. Different rows indicate the selectivity to the basic stimulus set, classified according to the number of stimulus classes that evoked responses: s, single; d, double; t, triple. Capital letters in the parentheses indicate the stimulus classes: P, planar; R, radial; C, circular. See the text for more details.

Fig. 13. Comparison of the responses to the plane stimulus sets between different directions of rotation. Three examples of neurons exhibiting different response patterns are shown. The left column indicates the responses to the stimuli in the preferred rotation and the right column indicates the responses to the stimuli in the

opposite (non-preferred) rotation. The scale for both these responses is at the bottom left in each row. Open circle represents excitatory response and solid circle represents inhibitory response. Other conventions are as in Fig. 7B. *A*: This neuron responded well to the stimuli in the preferred rotation but not to the stimuli in the non-preferred rotation. *B*: This neuron responded equally to both directions of rotation. *C*: This neuron responded to the stimuli in the non-preferred rotation but the response was limited only to a sub-set of the stimuli that caused responses in the preferred rotation.

Fig. 14. *A*: Distribution of the difference between the preferred tilt obtained from the clockwise rotating stimuli and that obtained from the anticlockwise rotating stimuli. The abscissa indicates difference in the preferred tilt, and the ordinate indicates the number of neurons. *B*: Distribution of the difference between the preferred slant obtained from the clockwise rotating stimuli and that from the anticlockwise rotating stimuli. In *A* and *B*, only neurons whose best response of all the non-preferred-rotation-stimuli was more than a half of the best response of all the preferred-rotation-stimuli and that exhibited selectivity in either of the rotations are included. Number of such neurons is indicated at the top right corner in each panel. Numbers in the parentheses are for neurons exhibiting significant selectivity in both rotations (filled bars). Both of the distributions in *A* and *B* have the peak at 0° indicating that many neurons preferred the same tilt and slant in both rotations.

Fig. 15. Schematic illustration to demonstrate that the selectivity to tilt and/or slant might be explained by the sensitivity to the local translational motion. Top rows indicate three plane stimuli with different simulated 3D-orientation. Bottom rows

indicate the local translational motion at the same position (squares) in the above stimuli. Stimuli with different simulated 3D-orientations contained different local translational motion at the same position in the stimuli.

Fig. 16. *A*: Schematic illustration of the alignment of the stimuli in the position invariance test. FP, fixation point; RF, receptive field. At five positions within the RF, I compared response to the optimum stimulus in the preferred rotation and response to the stimulus with the same tilt and slant in the non-preferred rotation. *B*: Example of responses of a neuron to the stimuli of the position invariance test. Filled and open bars indicate responses to the stimuli in clockwise and anticlockwise rotation, respectively. C, clockwise; A, anticlockwise. The height of bar indicates the response amplitude. Positions of bars correspond to the five different positions of the stimulus presentation. The response of this neuron was much stronger to the clockwise stimulus than to the anticlockwise stimulus at every position tested. *C*: Distribution of position invariance index for 24 neurons. The position invariance index was calculated by dividing direction selectivity index obtained at each peripheral position by that obtained at the central position. Because there are four pairs of a central position and peripheral positions for each neuron, four data from each of the 24 neurons contributed to this graph. Three pairs from three neurons were excluded from this analysis because no significance response was obtained to both the preferred and non-preferred rotation stimuli in these cases. So, a total of 93 pairs of responses are included in this analysis. The position invariance index was distributed around unity indicating that most neurons exhibited position invariance. See the text for more details.

Fig. 17. The selectivity to tilt and/or slant might be explained by the sensitivity to the speed of the moving dots. *A*: Top rows are schematic illustration of the four plane stimuli with different slants and the same tilt (0°). Bottom rows indicate the tangential speeds of moving dots at several positions along the vertical dashed lines in the above stimuli illustration. The length of arrows represents the speed of moving dots. The maximum or average speed as well as the magnitude of the speed gradient contained in the stimuli increased with the increase of slant. *B*: Distribution of the speed contained in the plane stimuli. The abscissa indicates the maximum speed contained in the plane stimulus and the ordinate indicates the rotating speed. Different lines represent different rotating speeds. Different symbols represent different slants.

Fig. 18. Responses of two slant selective neurons to the stimuli with three different rotation speeds. To examine the possibility that the slant selectivity is simply due to the sensitivity to speed or speed gradients, slant selectivity was tested using three different rotation speeds. The abscissa indicates the slant of the stimulus (left column) or the maximum speed in the stimulus (right column) and the ordinates indicate the amplitude of the response. Different symbols represent different rotation speeds as indicated in the inset. Error bars are standard deviations. *A*: This neuron exhibited similar responses to the stimuli at any rotation speed (left panel). *B*: This neuron exhibited a shift of the offset of the responses depending on rotation speed. The pattern of the slant selectivity was almost the same across different rotation speeds (left panel). Although the response gain or offset changed depending on rotation speed, this change could not be explained solely by the change in the speed or the speed gradients

in the stimuli (right column).

Fig. 19. An example of the control experiment using shuffled stimuli. Responses of a tilt selective neuron to the plane stimuli and the shuffled stimuli. The left column indicates the responses to the plane stimuli and the right column indicates the responses to the shuffled stimuli. The scale for both these responses is at the bottom left. Other conventions are as in Fig. 13. This neuron responded well to the plane stimuli and showed significant selectivity to tilt, but it did not respond to the shuffled stimuli.

Fig. 20. Schematic illustration of the processes that forms sensitivity to the plane stimuli. Conventions are as in Fig. 1.

Fig. 1

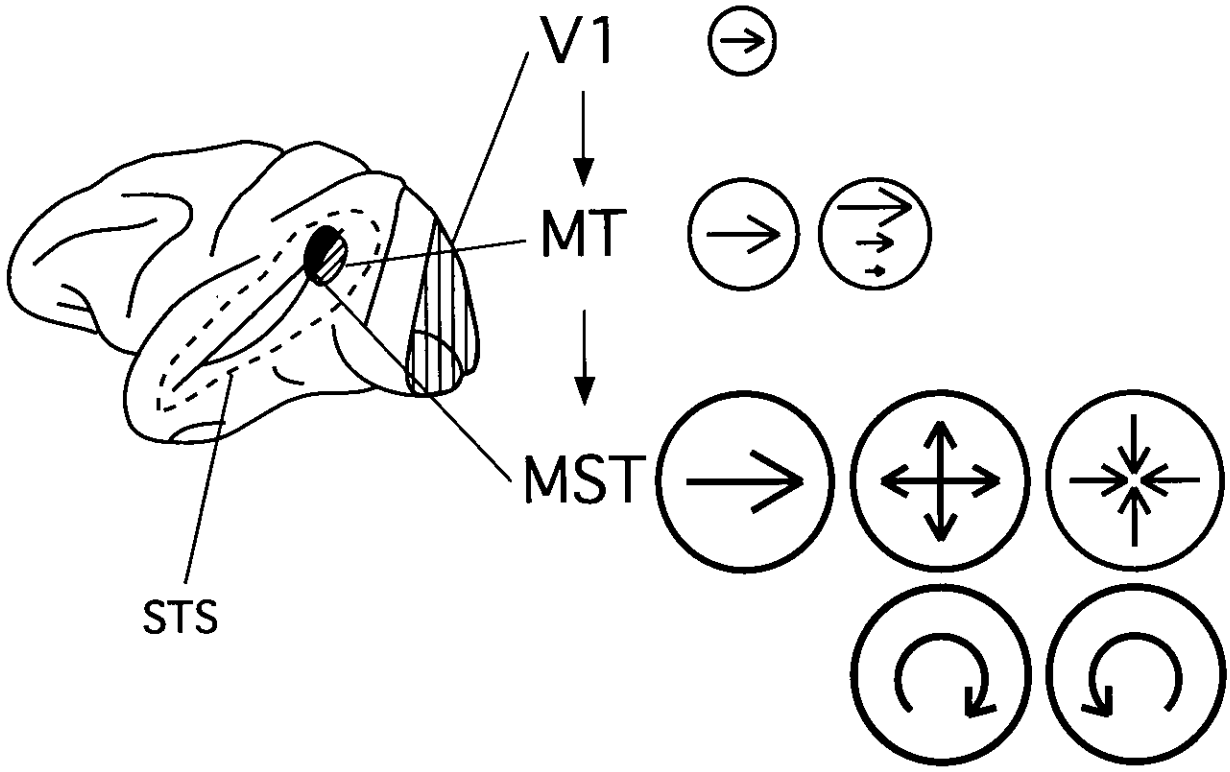

Fig. 2

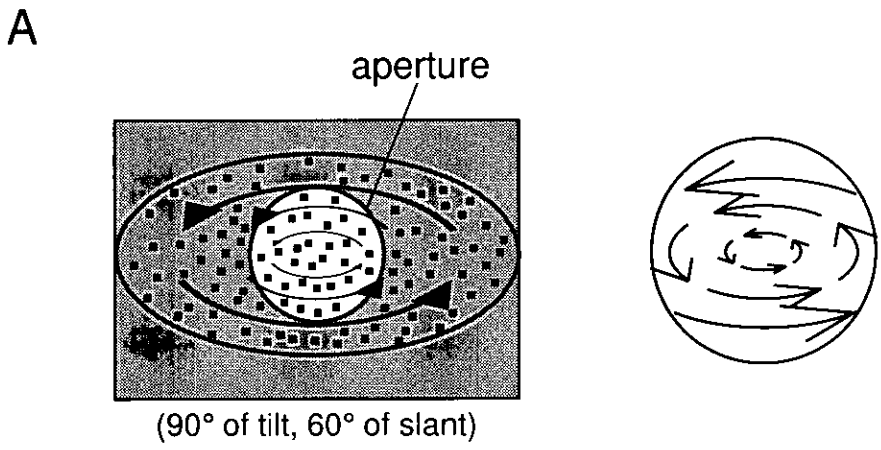
A
aperture
(90° of tilt, 60° of slant)
B
Slant
Tilt
C
tilt
90
135
45
0
20
40
60
slant

Fig. 3

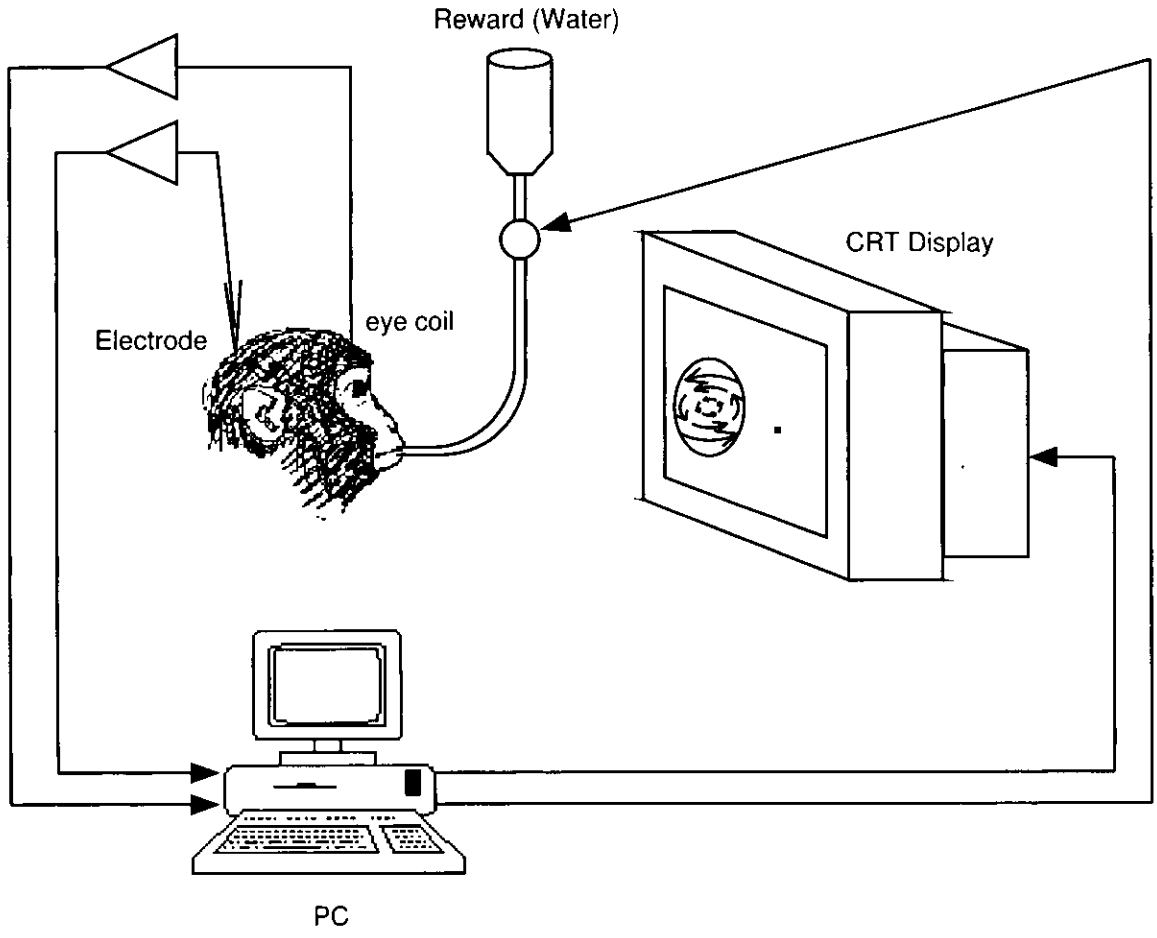

Fig. 4

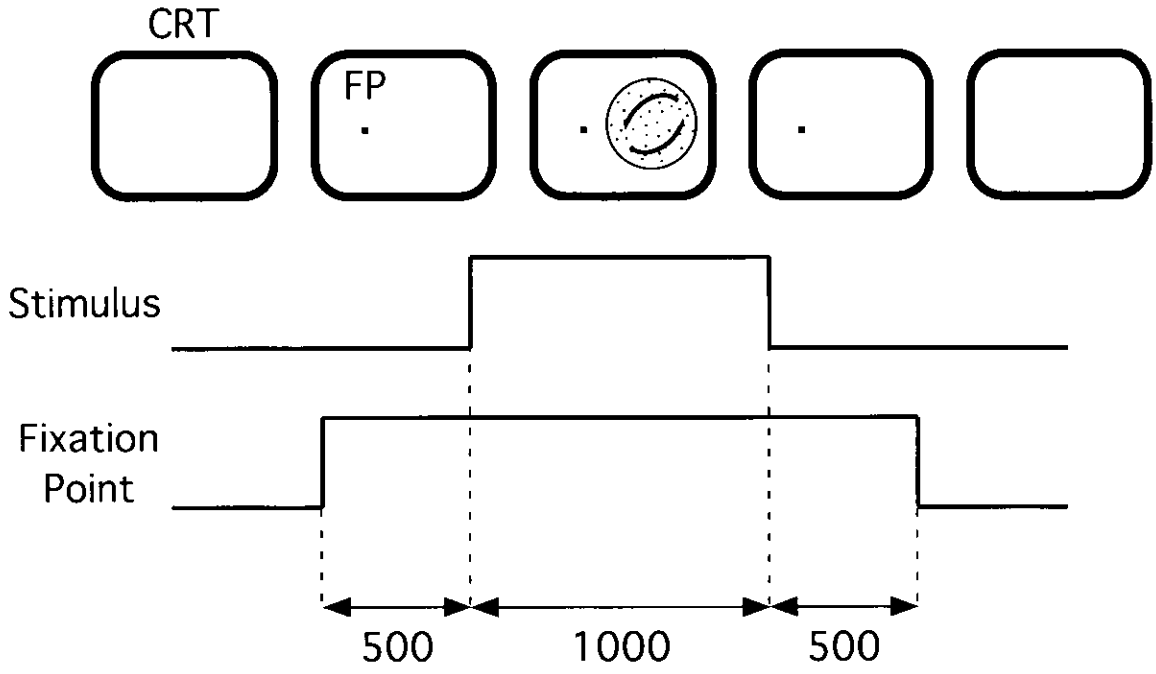

Fig. 5

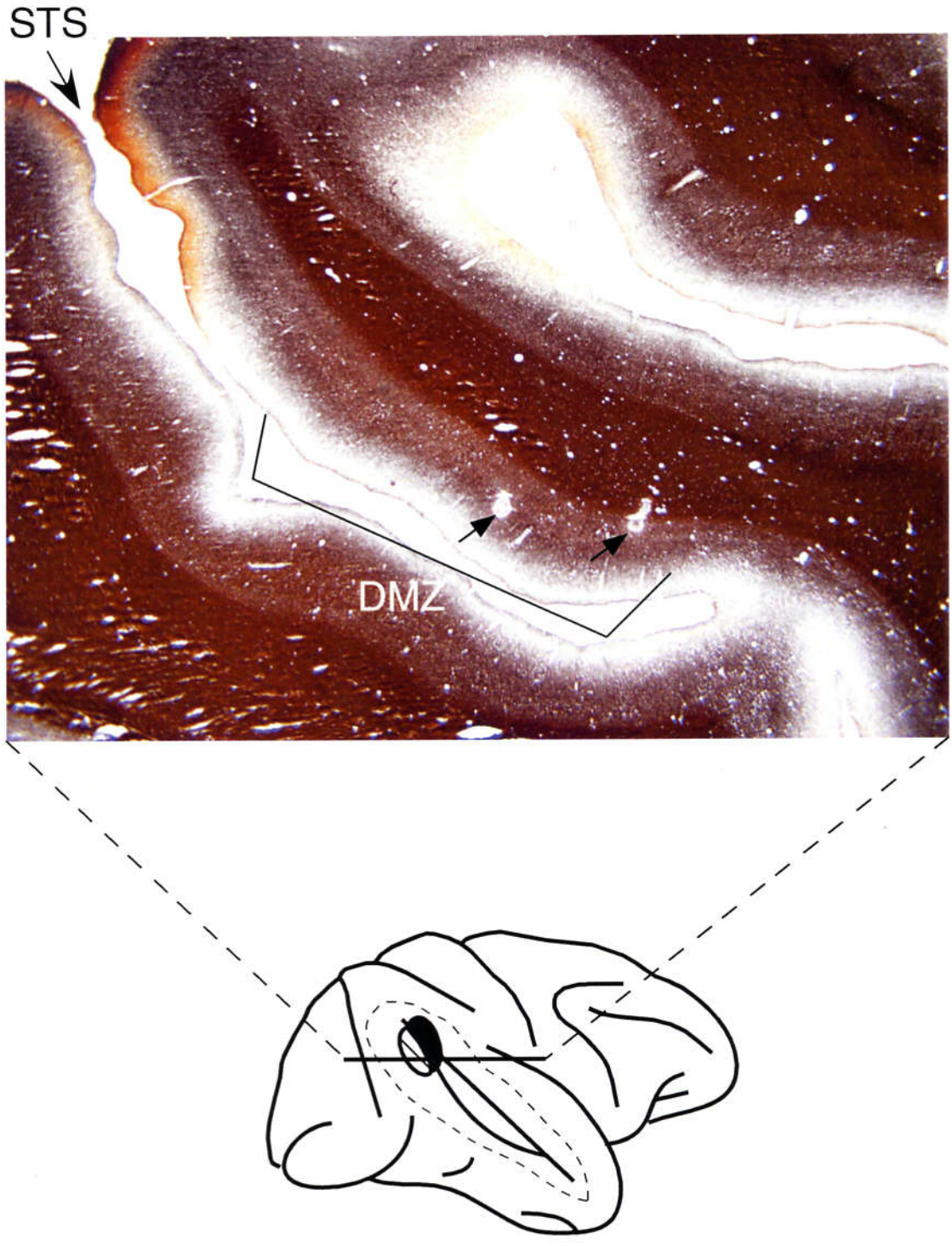

Fig. 6

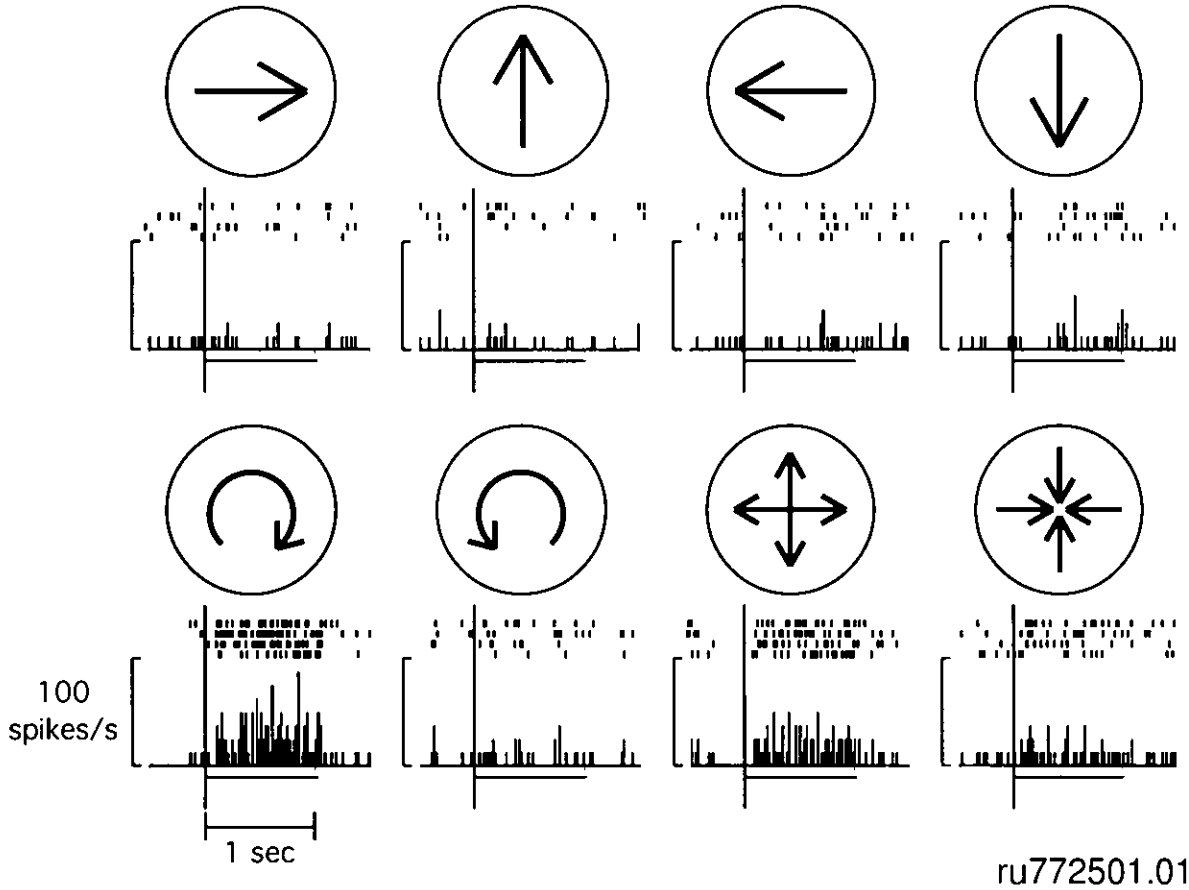

Fig. 7

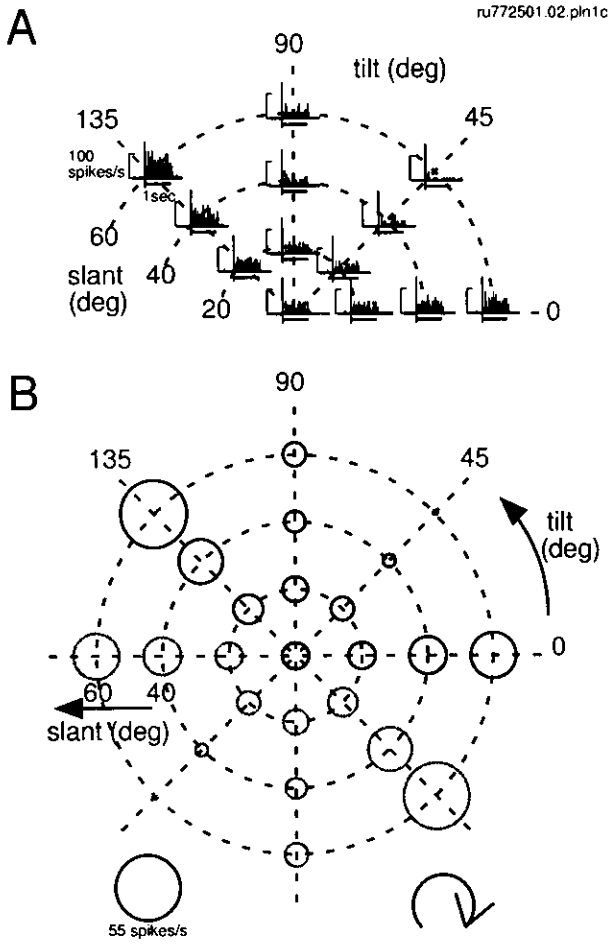
A
ru772501.02.pln1c
90
tilt (deg)
135
45
100
spikes/s
1sec
60
slant
(deg)
40
20
0
B
90
135
45
tilt
(deg)
0
60
40
slant (deg)
55 spikes/s

Fig. 8

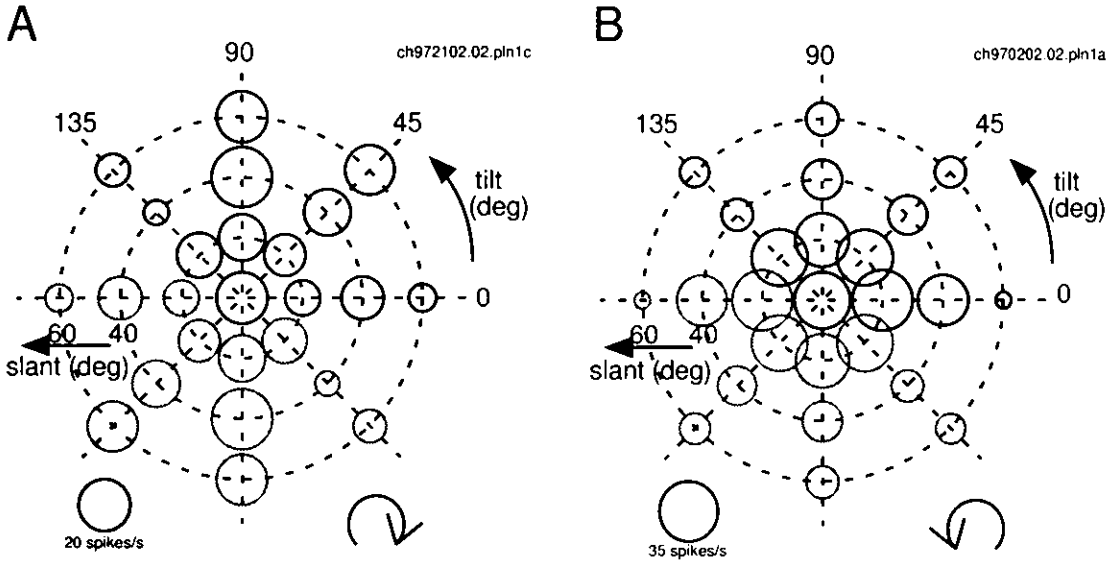
A
90
ch972102.02.pln1c
135
45
tilt
(deg)
0
60
40
slant (deg)
20 spikes/s
B
90
ch970202.02.pln1a
135
45
tilt
(deg)
0
60
40
slant (deg)
35 spikes/s

Fig. 9

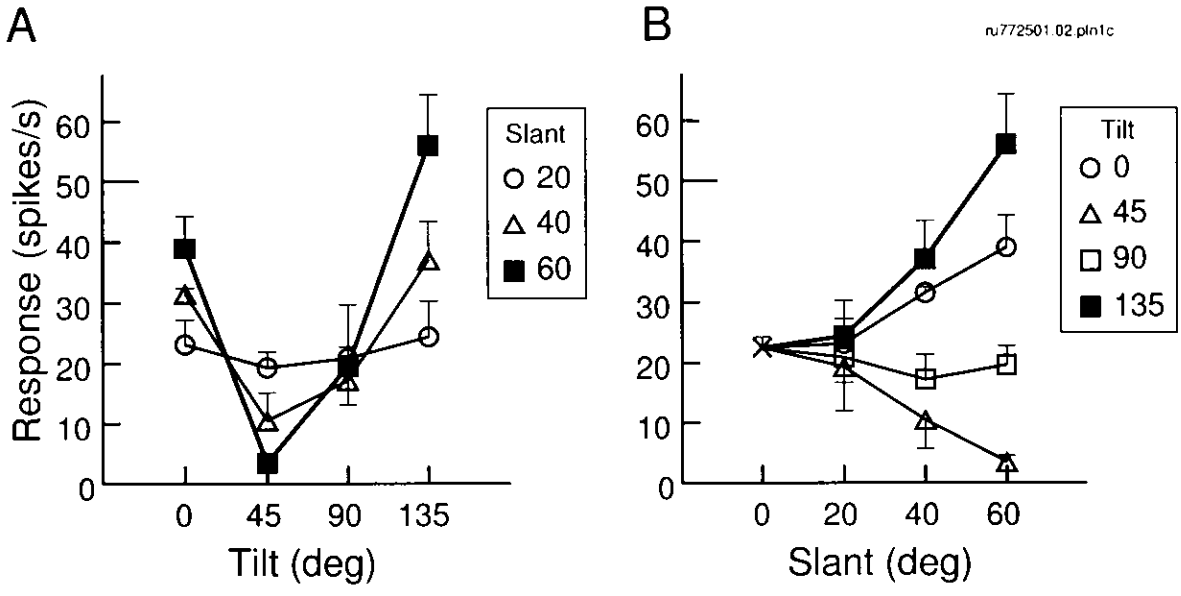
A
Response (spikes/s)
0
10
20
30
40
50
60
0
45
90
135
Tilt (deg)
Slant
20
40
60
B
ru772501.02.pln1c
0
10
20
30
40
50
60
0
20
40
60
Slant (deg)
Tilt
0
45
90
135

Fig. 10

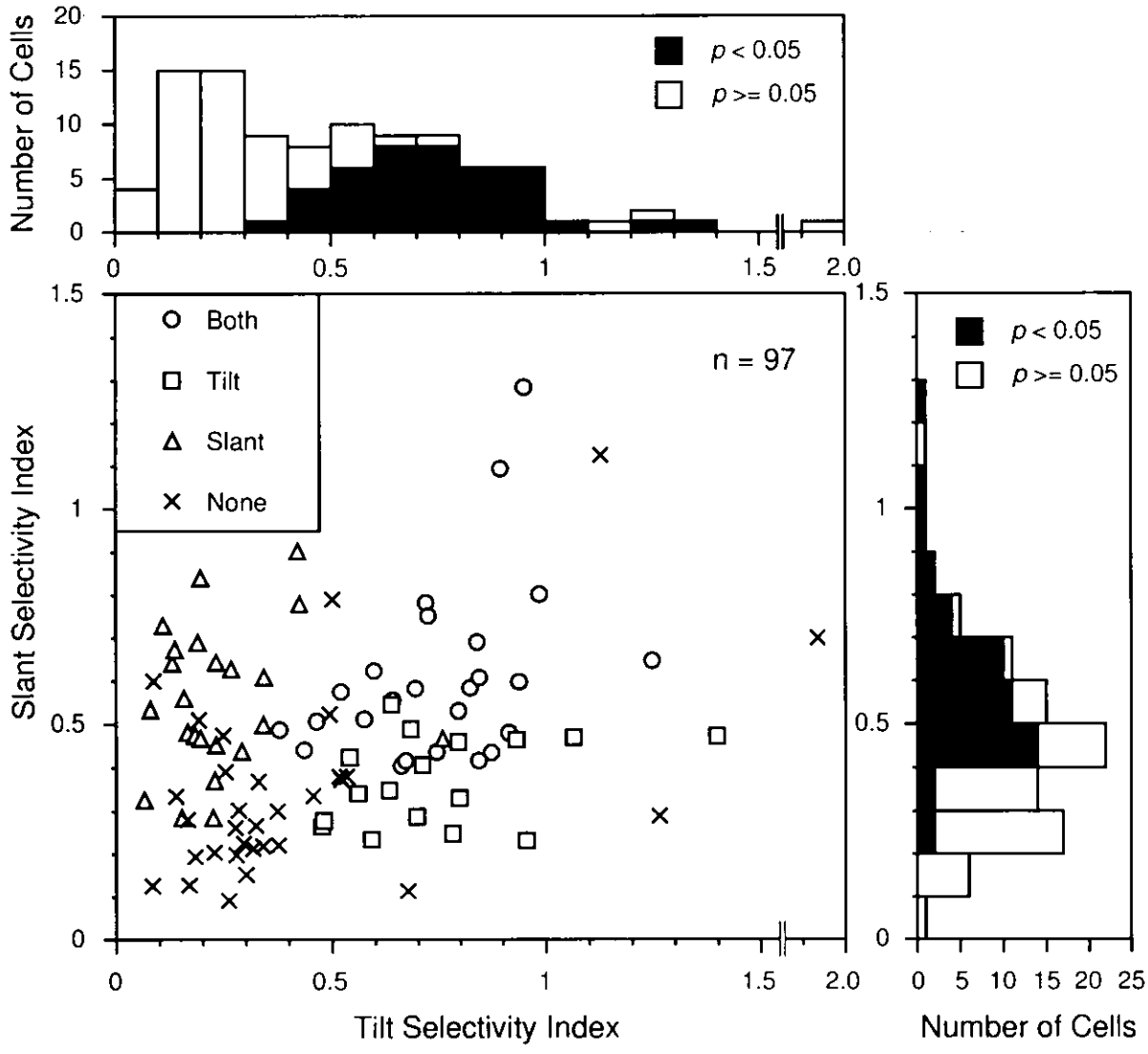
Number of Cells
20
15
10
5
0
0
0.5
1
1.5
2.0
p < 0.05
p >= 0.05
Both
Tilt
Slant
None
n = 97
Slant Selectivity Index
1.5
1
0.5
0
Tilt Selectivity Index
0 5 10 15 20 25
Number of Cells

Fig. 11

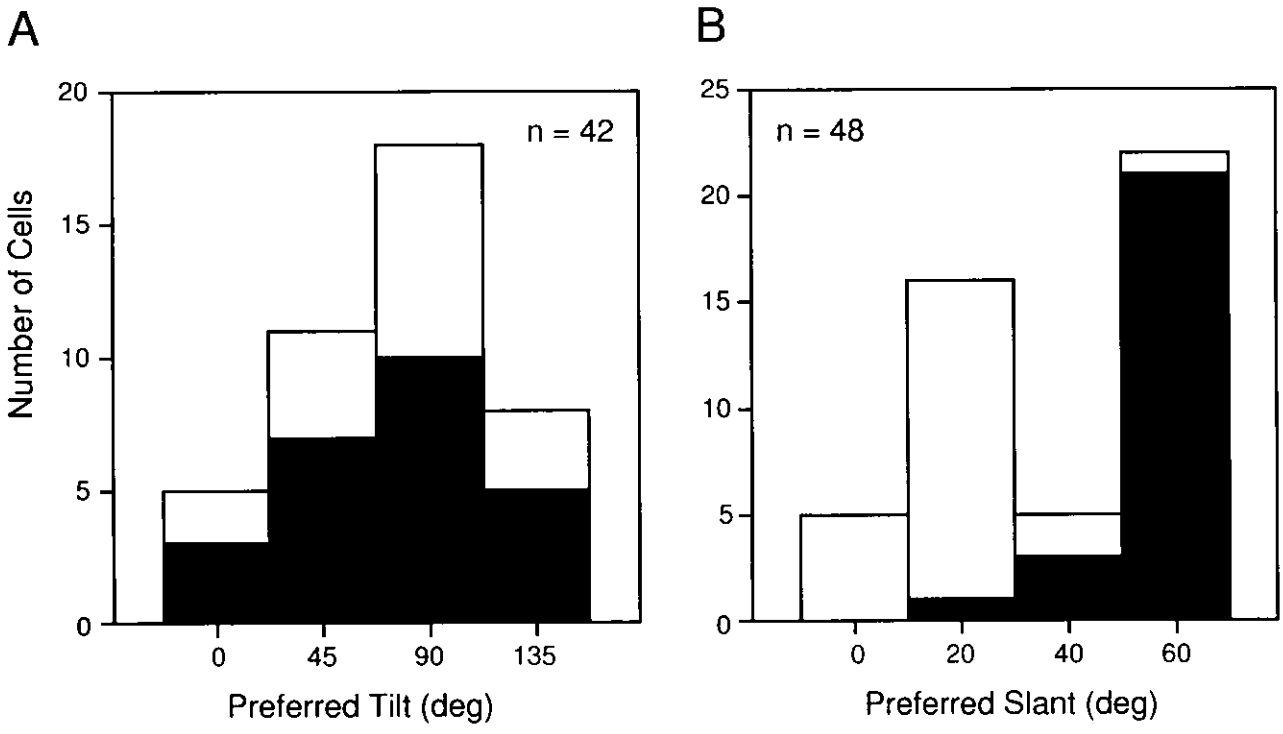
A
B
n = 42
n = 48
Number of Cells
Preferred Tilt (deg)
Preferred Slant (deg)
0
5
10
15
20
25
0
45
90
135
0
20
40
60

Fig. 12

	both	tilt	slant	none	total
s $\begin{pmatrix} P \\ R \\ C \end{pmatrix}$	6 $\begin{pmatrix} 4 \\ 1 \\ 1 \end{pmatrix}$	6 $\begin{pmatrix} 1 \\ 1 \\ 4 \end{pmatrix}$	15 $\begin{pmatrix} 0 \\ 0 \\ 15 \end{pmatrix}$	15 $\begin{pmatrix} 4 \\ 1 \\ 10 \end{pmatrix}$	42 $\begin{pmatrix} 9 \\ 3 \\ 30 \end{pmatrix}$
d $\begin{pmatrix} PR \\ PC \\ CR \end{pmatrix}$	13 $\begin{pmatrix} 7 \\ 3 \\ 3 \end{pmatrix}$	7 $\begin{pmatrix} 2 \\ 3 \\ 2 \end{pmatrix}$	3 $\begin{pmatrix} 0 \\ 1 \\ 2 \end{pmatrix}$	7 $\begin{pmatrix} 2 \\ 5 \\ 0 \end{pmatrix}$	30 $\begin{pmatrix} 11 \\ 12 \\ 7 \end{pmatrix}$
t	6	4	5	10	25
total	25	17	23	32	97

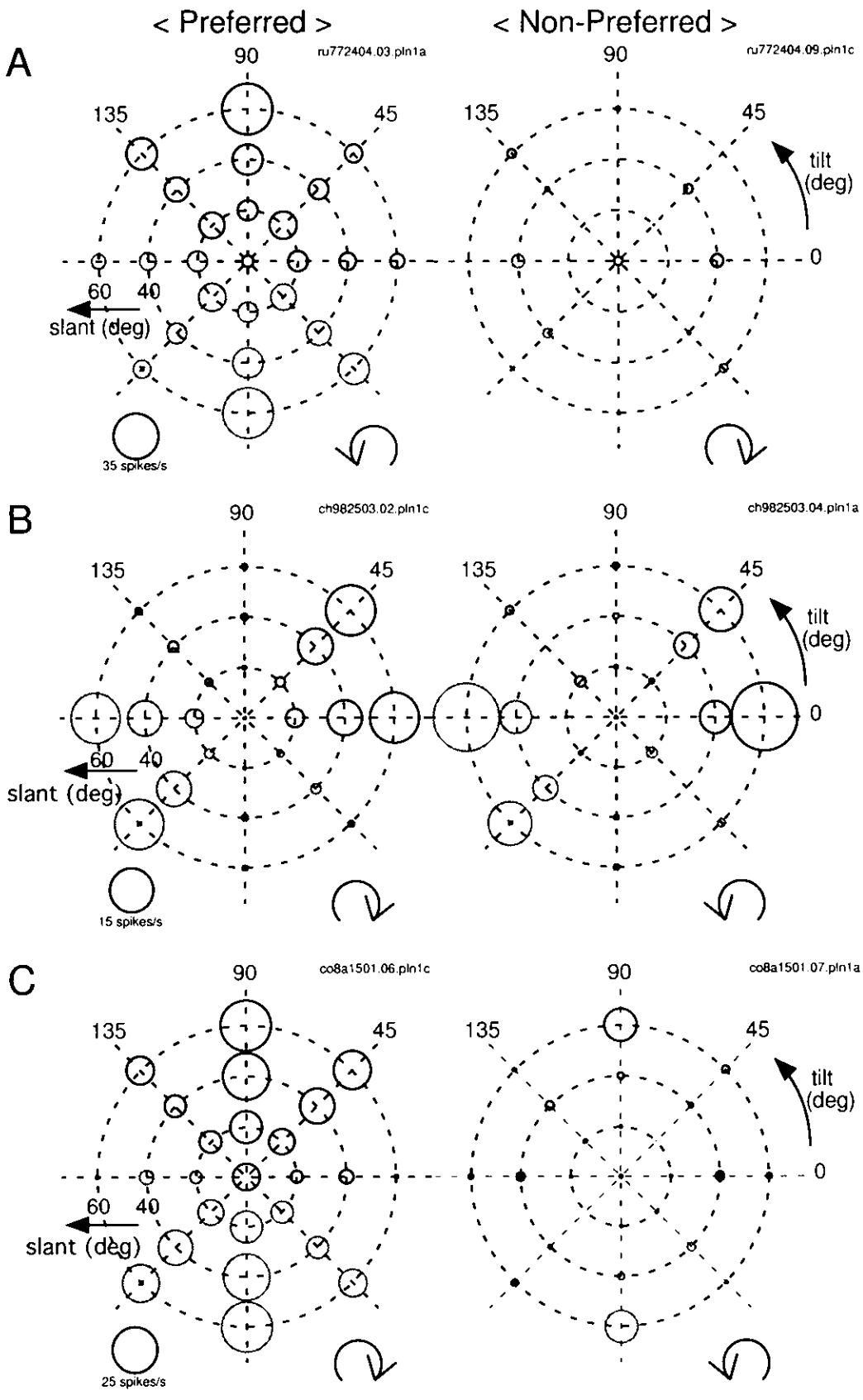
< Preferred >
< Non-Preferred >
A
ru772404.03.pln1a
ru772404.09.pln1c
90
135
45
0
tilt
(deg)
60
40
slant (deg)
35 spikes/s
B
ch982503.02.pln1c
ch982503.04.pln1a
15 spikes/s
C
co8a1501.06.pln1c
co8a1501.07.pln1a
25 spikes/s

Fig. 14

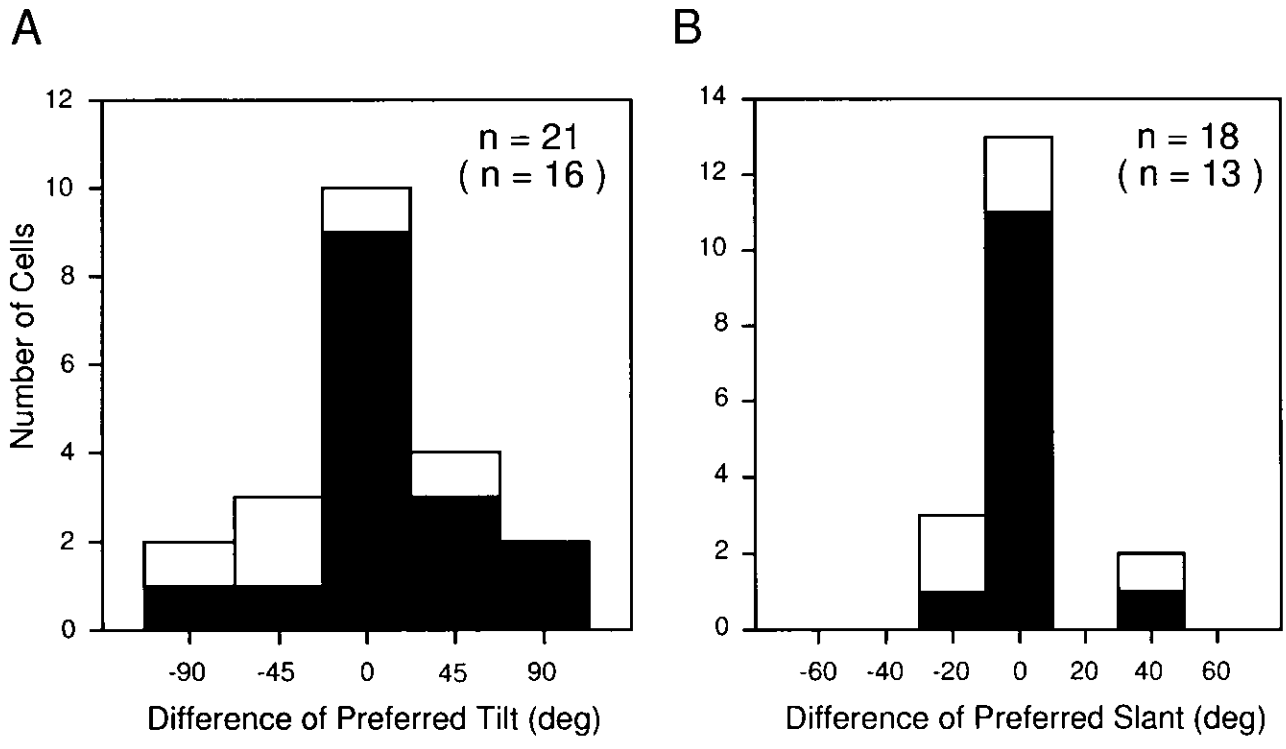
A
B
n = 21
(n = 16)
n = 18
(n = 13)
Number of Cells
Difference of Preferred Tilt (deg)
Difference of Preferred Slant (deg)
0
2
4
6
8
10
12
14
-90
-45
0
45
90
-60
-40
-20
0
20
40
60

Fig. 15

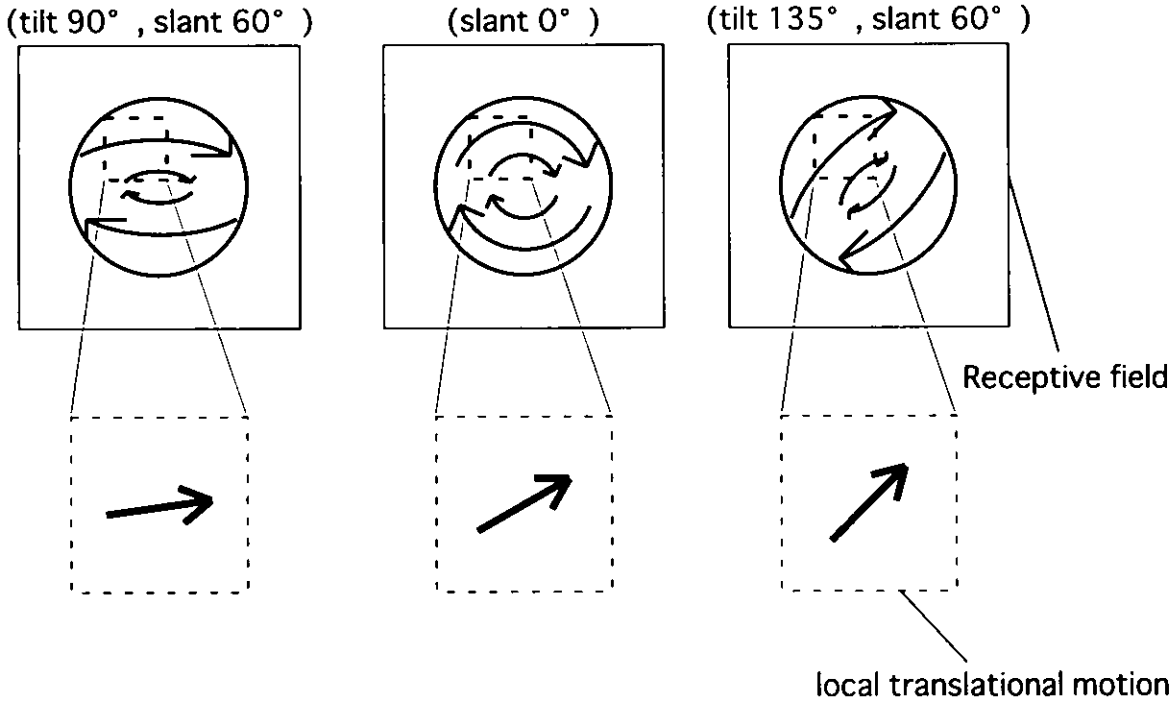
(tilt 90° , slant 60°)
(slant 0°)
(tilt 135° , slant 60°)
Receptive field
local translational motion

Fig. 16

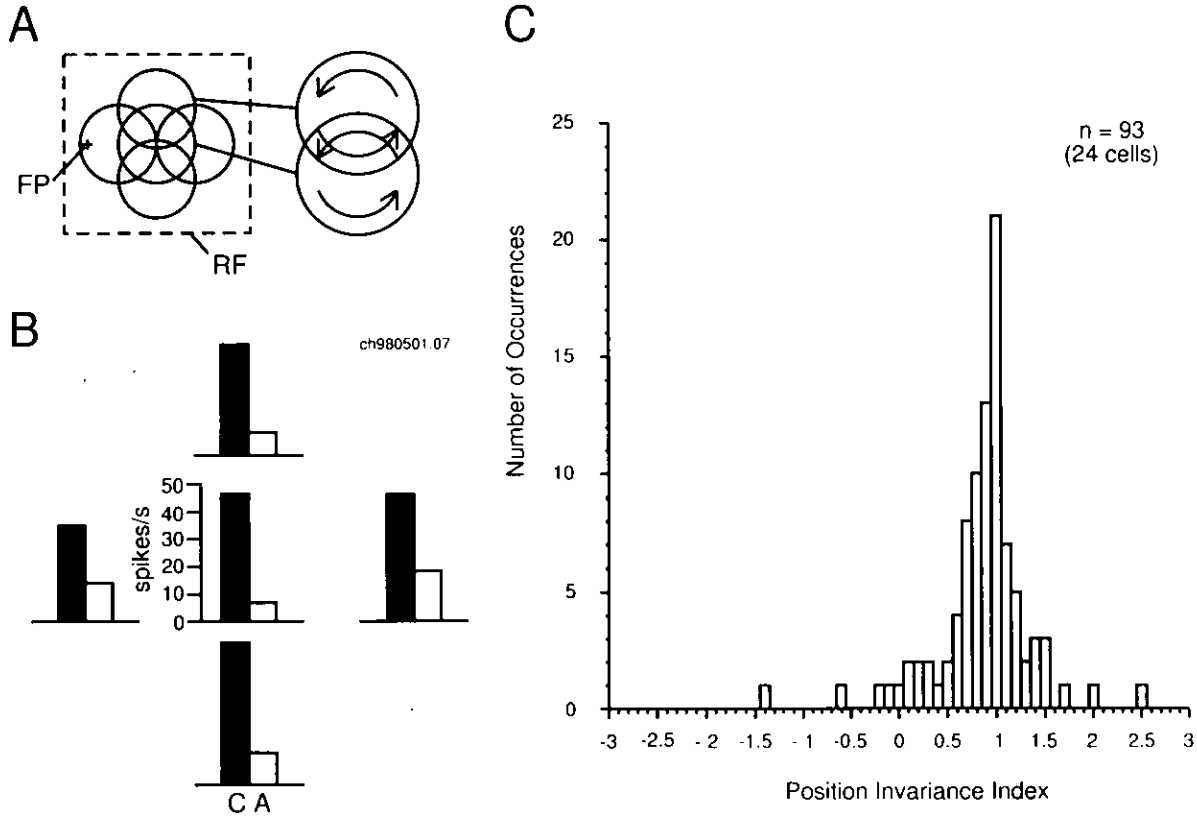
A
FP
RF
B
ch980501.07
spikes/s
50
40
30
20
10
0
C A
C
n = 93
(24 cells)
Number of Occurrences
25
20
15
10
5
0
-3
-2.5
-2
-1.5
-1
-0.5
0
0.5
1
1.5
2
2.5
3
Position Invariance Index

A

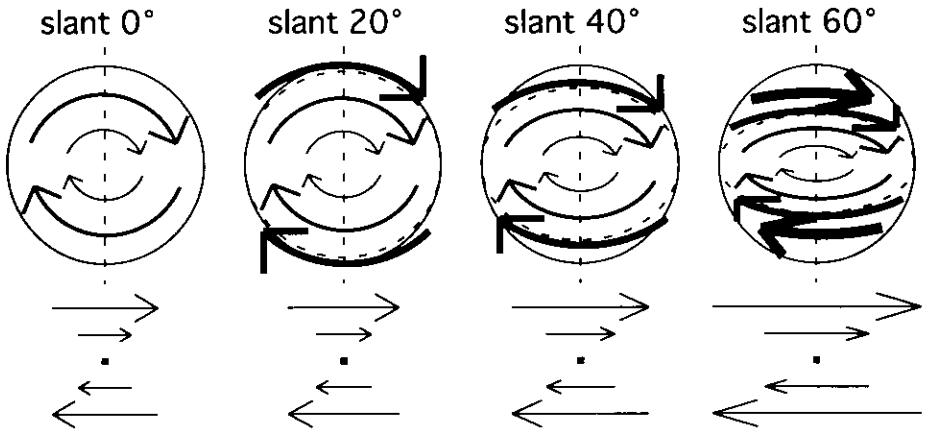
slant 0°
slant 20°
slant 40°
slant 60°

B

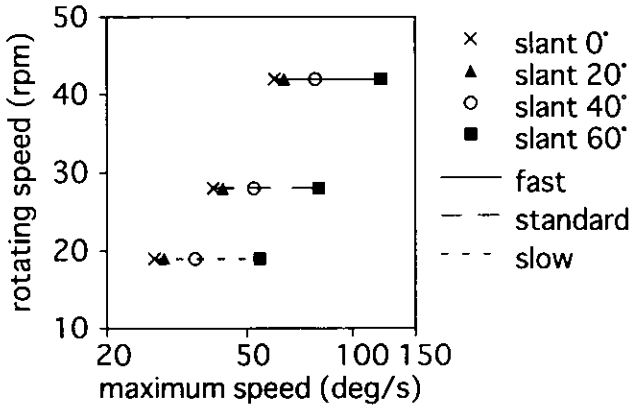
50
40
30
20
10
rotating speed (rpm)
20
50
100 150
maximum speed (deg/s)
slant 0°
slant 20°
slant 40°
slant 60°
fast
standard
slow

Fig. 18

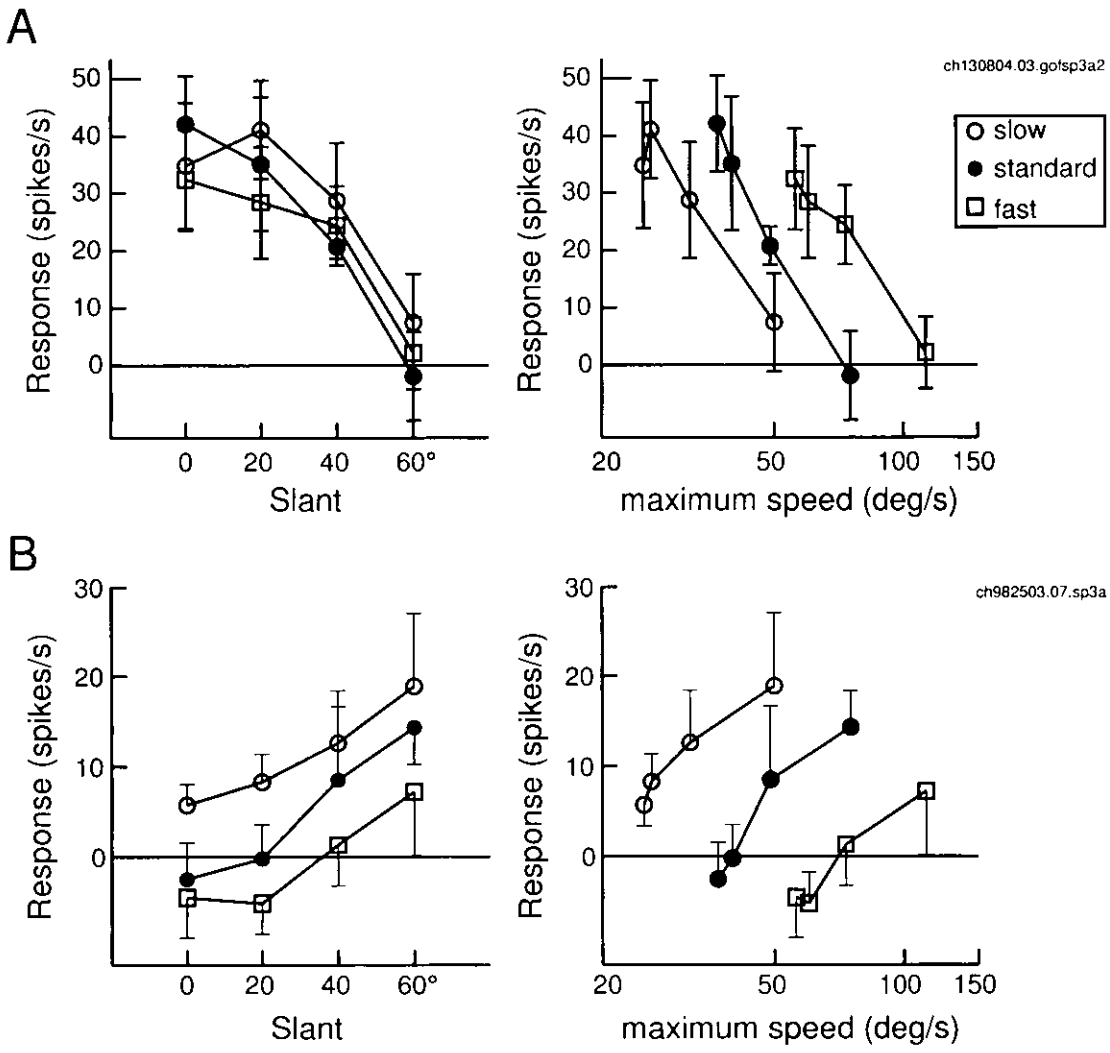
A
ch130804.03.gofsp3a2
slow
standard
fast
Response (spikes/s)
50
40
30
20
10
0
0
20
40
60°
Slant
20
50
100
150
maximum speed (deg/s)
B
ch982503.07.sp3a
30
20
10
0
Response (spikes/s)
Slant
maximum speed (deg/s)

Fig. 19

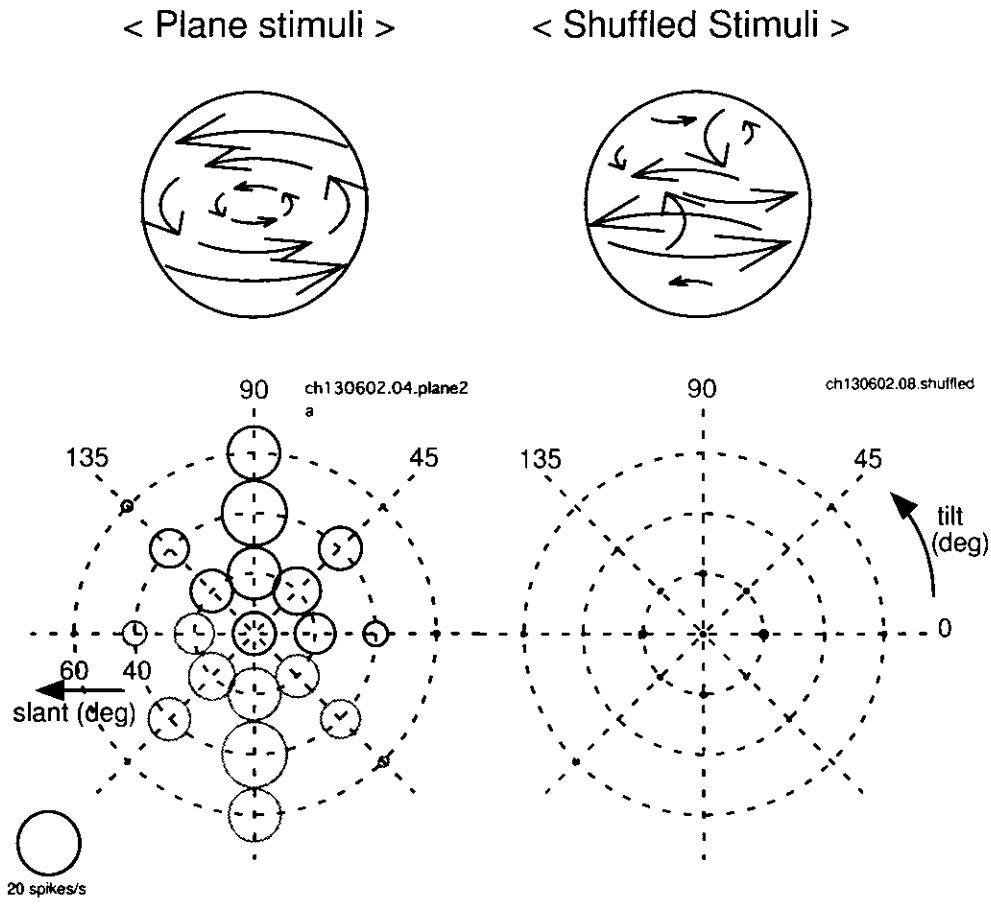
< Plane stimuli >
< Shuffled Stimuli >
90
ch130602.04.plane2
a
135
45
60
40
slant (deg)
20 spikes/s
90
ch130602.08.shuffled
135
45
tilt
(deg)
0

Fig. 20